



저작자표시-비영리-변경금지 2.0 대한민국

이용자는 아래의 조건을 따르는 경우에 한하여 자유롭게

- 이 저작물을 복제, 배포, 전송, 전시, 공연 및 방송할 수 있습니다.

다음과 같은 조건을 따라야 합니다:



저작자표시. 귀하는 원저작자를 표시하여야 합니다.



비영리. 귀하는 이 저작물을 영리 목적으로 이용할 수 없습니다.



변경금지. 귀하는 이 저작물을 개작, 변형 또는 가공할 수 없습니다.

- 귀하는, 이 저작물의 재이용이나 배포의 경우, 이 저작물에 적용된 이용허락조건을 명확하게 나타내어야 합니다.
- 저작권자로부터 별도의 허가를 받으면 이러한 조건들은 적용되지 않습니다.

저작권법에 따른 이용자의 권리는 위의 내용에 의하여 영향을 받지 않습니다.

이것은 [이용허락규약\(Legal Code\)](#)을 이해하기 쉽게 요약한 것입니다.

[Disclaimer](#)

공학박사 학위논문

Multiplex Colorimetric Diagnosis for Point of Care Test Using Encoded Microparticle

코드화된 미세입자를 이용한 색기반의 동시다발적 현장
진단 플랫폼 개발

2019 년 2 월

서울대학교 대학원

전기컴퓨터 공학부

정 윤 진

Abstract

Multiplex Colorimetric Diagnosis for Point of Care Test Using Encoded Microparticle

Yunjin Jeong
Department of Electrical and Computer Engineering
The Graduate School
Seoul National University

In this dissertation, a multiplex colorimetric diagnosis platform using encoded microparticles is proposed. Multiple target biomolecules can be detected by an office scanner as a concept of point of care tests within low-resource settings. The encoded microparticles guarantee high multiplexing capacity up to millions. Detection using gold nanoparticles in platform was demonstrated with assay results according to the color change of the encoded microparticles. Realizing scanner-based multiplex assay, this platform's novelty lies in fabrication of the encoded particles with two materials and introduction of a signal enhancement step to the multiplex bead-based assay using deposition of gold for higher sensitivity.

The encoded microparticles, in which the engraved codes indicate the types of target molecules, are prepared to capture target. The design of the particles including the size and the materials were determined, to analyze the assay results

with images taken by scanners. Also, the high-throughput fabrication methods have been developed to guarantee that more than 1000 particles can be fabricated in less than 3 minutes. The encoded particles with a single code are coated by silica and chemically conjugated to one type of capture molecules. This pairing guarantees the code to indicate the type of target molecules in multiplexing assay. The encoded microparticles targeting various molecules are pooled and reacted to samples with target molecules. After capturing targets on the multiple types of encoded particles, the particles conjugated with targets react with detection molecules. The detection molecules include gold nanoparticles to change the levels of target molecules into color signals. If the signal is too weak, a signal enhancement step is introduced using gold deposition to the seed gold nanoparticles with targets. After the whole colorimetric assay, the reacted particles are imaged using an office scanner, from which the code and the assay results are analyzed using image processing. The size of the microparticles was considered according to the proper resolution of the scanners. To be applied to various situations, two types of particles have been developed and utilized. 900 μm particles with 2.5 million kinds of character codes and 300 μm particles with 70-256 kinds of binary codes are developed to be scanned with 1200 and 4800 dpi respectively.

As a proof of concept to show a wide range of applications, proteins and genes are detected. Using 4-plex assay, multiple sclerosis autoimmune disease patients

are classified from healthy people with $p < 0.0001$ in an unpaired t-test. Using 3-plex assay, bacterial meningitis genes are detected within 1000 molecules.

This scanner-based assay platform can expand the clinical impacts of the multiplex assay. This platform can be applied to various circumstances where high-resource settings have not been set. With operators and scanners, the platform can be applied to multiplex assay in high multiplexing capacity and high throughput.

Keywords: multiplex colorimetric assay, point-of-care test, encoded microparticle, office scanner, diagnosis with immunoassay or genotyping

Student Number: 2013-20880

Table of Contents

ABSTRACT	I
MULTIPLEX COLORIMETRIC DIAGNOSIS FOR POINT OF CARE TEST USING ENCODED MICROPARTICLE	I
TABLE OF CONTENTS	IV
LIST OF TABLES.....	VIII
LIST OF FIGURES	IX
CHAPTER 1. INTRODUCTION.....	1
1.1. Multiplex point of care test	2
1.1.1. Multiplex assay for diagnosis of patients	2
1.1.2. Needs of multiplex point of care test near to patients	5
1.2. Main Concept: Multiplex colorimetric assay platform with encoded microparticle.....	8
1.2.1. Multiplex colorimetric assay platform with encoded microparticle	9
1.2.2. Advantages of scanner as widely spread detecting device	10

1.2.3. Core technology of platform	1 2
1.3. Outline of dissertation	1 8
CHAPTER 2. BACKGROUND	1 9
2.1. Process of multiplex assay	2 0
2.2. Previous multiplex point of care technology	2 1
2.2.1. Technology for multiplex point of care test technology	2 2
2.2.2. Positioning of previous technology for multiplex assay	2 9
2.3. Commercialized multiplex assay devices for point of care test	3 1
2.3.1. Pros and cons of conventional automated machines for multiplex point of care test	3 8
2.4. Previous research in the group	4 3
CHAPTER 3. PLATFORM DEVELOPMENT.....	4 6
3.1. Preparing process of encoded microparticle conjugated with capture molecule	4 7
3.1.1. Particle design considerations for scanner-based detection	4 9
3.1.2. Fabrication process of dual-functional encoded particle.....	5 2
3.1.3. Strategy to fabricate dual-functional sequentially with fixing polymers at the same position.....	5 5
3.1.4. High-throughput fabrication method	5 7
3.1.5. Process of chemically conjugating capture molecules on surface of encoded particles	6 4
3.2. Process of massively parallel multiplex colorimetric assay	6 7

3.3. Optimization of imaging process with office scanner.....	6 8
3.3.1. Optimization of imaging plate.....	6 9
3.3.2. Optimization of resolution of scanning.....	7 0
3.4. Data analyzing process	7 1
3.4.1. Particle detection and alignment process.....	7 2
3.4.2. Algorithm for decoding particles and analyzing results of colorimetric assay from scanned images.....	7 4
CHAPTER 4. PLATFORM VALIDATION WITH APPLICATION:	
ANTIBODY FROM AUTOIMMUNE DISEASE AND GENE FROM BACTERIAL MENINGITIS.....	7 8
4.1. Validation for immunoassay with autoimmune disease samples.....	7 9
4.2. Validation for genotyping with bacterial meningitis target.....	8 7
CHAPTER 5. CONCLUSION AND DISCUSSION.....	9 1
5.1. Summary of dissertation	9 2
5.2. Comparison with previous technology	9 4
5.3. Limit of platform.....	9 7
5.4. Future work.....	9 9
BIBLIOGRAPHY	1 0 0

국문 초록 1 1 0

List of Tables

Table 2.1 Comparison between previously developed technologies [40], [47], [54], [67]–[74]. Representative properties are noted because each technique has edited versions where the characteristics are different with compensation between the topics according to applications.....	3 1
Table 2.2 Characteristics of automated multiplex assay devices with commercialization [29]–[32], [77].	4 0
Table 2.3 Information of conventionally developed machine for multiplex POCT of protein [29].....	4 1
Table 2.4 Estimated prices of Verigene® and Filmarray® with considering maximum throughput per day [30], [31].....	4 2
Table 3.1 Comparison of fabricating time among the various fabrication methods.	6 4
Table 5.1 Spec of developed encoded particles in this dissertation.	9 3

List of Figures

- Figure 1.1 Detection process of target biomolecules in blood. Biomolecules include antibodies, antigens, RNAs and DNAs. The target molecules are detected with sequential biochemical reactions with capture molecules, target molecules and detection molecules. Target molecules can be quantified or typed with on-off detection..... 3
- Figure 1.2 Schematic for indicating global locations where infectious diseases are emerged or re-emerged. Red dots indicate the locations where new diseases emerged, blue dots indicate the locations where diseases re-emerged or resurged and black dots indicate the locations where diseases emerge deliberately [23], [25]..... 7
- Figure 1.3 Schematic of system for scanner-based multiplex colorimetric assay with encoded microparticles. The encoded microparticles are conjugated with different targets via the codes. The encoded microparticles are pooled together and biochemically reacted in a tube with a sample including targets. Finally, the reacted particles are scanned on an office scanner [28]..... 9
- Figure 1.4 Comparison between smartphone and office scanner. Smartphone system needs additional devices such as a lens and a focusing system. There are pros and cons of the devices. Pros are noted in blue and cons are noted in red..... 12
- Figure 1.5 Microscope images and schematic of lateral view for before and after colorimetric assay with condensation of gold on 50 um bead. The code of the particle is a groove form which

is not holes. The condensation of gold is to enhance the optical color change in order to detect molecules with higher sensitivity. The condensation of gold inhibits code to be identified in bright field image from a microscope. 1 4

Figure 1.6 Schematic of particle consisting of dual functional materials. The particle is composed of two regions: an analysis region and an encoding region. Capture molecules are conjugated on all the regions but analyzing is performed with only on the transparent analysis region which has a weak color backgrounds. The encoding region is colored so easily detectable with scanning from office scanners without additional devices. 1 6

Figure 1.7 Schematic of signal enhancement step using condensation of gold around the seed nanoparticles conjugated to the surface of the encoded particles. The seed nanoparticles are conjugated on the encoded microparticles after colorimetric assay, but the visible color change is not enough to be imaged by an office scanner. With a signal enhancement step using gold condensation, the visible color of encoded microparticles changes more dramatically to be detected by the scanned images. 1 7

Figure 2.1 Schematic of design and protocol of paper-based test from blood. The device is operation-free in the multiplex assay from a drop of human blood. This paper has five detection zones, and each target is quantified by color in each zone. The paper consists of two layers of papers. One is a plasma separation membrane, and the other is a laminated cover of a polyester film where patterned hydrophobic channels are integrated. A drop of whole blood which is around 30 μ l is necessary for quantification of multiple targets. In the plasma

separation membrane, blood cells are filtered out, so only plasma can pass through. The test takes around 15 minutes, and the results are matched through the color guide. [47]...	2 4
Figure 2.2 Schematic of a microfluidic platform which integrates sequential and parallel steps for detecting multiple analytes [58].....	2 6
Figure 2.3 Design of lab-on-a-disc which includes various steps for detecting target biomarkers. Centrifugal force works as a power source of fluid and a valve controller [59].	2 6
Figure 2.4 Basic principles of bead-based immunoassay for multiplex colorimetric assay. The microbeads have a different degree of fluorescence as a label for the capture antibody. The tagged detection antibody indicates the existence of the analyte connected to the microbeads [66].	2 8
Figure 2.5 Type and detecting process of microbeads conjugated with target biomarkers for multiplex assays. Code and level of biomarker are detected in a fluorescent flow cytometer approach or fluorescent imaging approach after assembled in a single layer by magnetic power [66].	2 8
Figure 2.6 Positioning of conventional technology for multiplex POCT. The accessibility of the platform and the information derived from the platform are considered critically. The axis of accessibility counts how high resources and how much operations are necessary. The axis of information counts the multiplexing capacity and the sensitivity [40].	3 0
Figure 2.7 Image of Ella® and schematic to show principle of Ella®. The Ella system uses the microfluidic system and detects multiple analytes in separated chambers. The valves are used to perform sequential reactions in the microfluidic channel. The final signal is detected in fluorescence.	3 3

Figure 2.8 Schematic of principle for Verigene® solid-phase microarray. The targets are conjugated with two types of components which are conjugated with target-specific capture molecules. The single-stranded capture molecules are immobilized on the specific position of microarray and particles. (A) The position of capture molecules in microarray indicates the targeting probes. The target probes are annealed to the complementary capture probes on the microarray. Other capture molecules which are targeting different regions of target molecules are conjugated to gold particles. So the gold nanospheres can be immobilized on the specific region of the microarray glass by annealing to the complementary targets. The whole chip is washed to remove unbound residues such as genes and gold particles. By condensation of metal materials, the optical sensitivity increases for detection with higher sensitivity. (B) Target-specific capture molecules are aligned and conjugated on the specific regions on purpose. Each kind of capture molecules is positioned in three different regions to be tested in triplicate for higher accuracy of results to be guaranteed. (C) Targets are detected in bright field images. A light source irradiates light across the array. Then, the optical camera can image the regions in a bright field with colorimetric results [77]. 3 5

Figure 2.9 Schematic of cartridge and principle used in the Filmarray® device. Physical lysis is performed in the first chamber to analyze various cells in blood including viruses, bacteria, yeast, and parasites. Then two-stage PCR is performed. The first PCR is multiplex PCR and the second PCR is a single set of PCR in separated microwells. Then, final results are imaged with fluorescent signals targeting secondly

amplified DNAs [30].....	3 7
Figure 2.10 Images and spec of commercialized Lumenex devices for fluorescent bead-based assay. The devices have different methods for imaging, and the multiplexing capacity differs by the type of machines [31].....	4 3
Figure 2.11 Schematic and images of multiplex HPV genotyping performed using encoded and silica-coated microparticles with shape codes. (a) A schematic explaining the process and principle of multiplex HPV genotyping using encoded silica-coated microparticles and streptavidin which is chemically conjugated with fluorescent molecules. Silica-coated microparticles are suitable for inhibiting unspecific binding to the particles. (b) A bright-field and a fluorescence microscopy image are shown after the assay for genotyping. The shape codes can be read within a bright-field image, but assay results should be read using a fluorescent image. In the fluorescent image, the particles with probes complementary to the target HPV 33 sequences show strong fluorescence. It is because only HPV 33 targets are used for the assay and it shows the availability of the platform as a genotyping tool [35].....	4 4
Figure 3.1 Schematic of the developing process of the scanner-based multiplex colorimetric assay platform. The process is preparing particles, performing the biochemical reaction, imaging with an office scanner and analyzing data from the image [28].....	4 7
Figure 3.2 Schematic of 900µm particles with character codes formed as holes. (a) Particles consist of two materials with different functions. One is a transparent part named as an analysis region which represents levels of target molecules as the color changes. The other is colored part named as an	

encoding region which indicates the target molecule. (b) The encoding region includes aligning key and code. The aligning key help to identify upside down form of the encoded particle.
 5 0

Figure 3.3 Schematic of 300 μm particles with binary codes formed as transparent regions. Particles consist of two materials with different colors. One is a transparent part, and the other is a colored part. The analysis region is not all transparent parts but only for centered transparent areas. It is because the transparent parts at the boundary show higher CV compared to the part at the center..... 5 1

Figure 3.4 Schematic and images for showing fabrication process of dual-functional particles. 900 μm particles are fabricated with two different mixtures. The particles have codes in hole formats. The codes consist of 4 characters. The images are from microscopy [28]. 5 4

Figure 3.5 Scanned images of 900 μm encoded dual-functional particles. The particles have four-length character codes and eight-length binary codes respectively. 5 4

Figure 3.6 Condensed structure of TMSPA. The chemical groups including Si increase the physical bonding with glass substrates during polymerization. 5 6

Figure 3.7 Schematic of oxygen inhibition layer derived near to PDMS during polymerization of PEG hydrogels. The oxygen layer is generated because PDMS is a gas permeable substrate. The oxygens absorb the chemically activated energy for polymerization, so the polymerization near the PDMS substrate is inhibited. Finally, the polymerized regions by UV light have weaker physical bonding force to PDMS substrate compared to the force to a glass substrate [88]. 5 7

Figure 3.8 Schematic for process of sequential polymerization with a single monomer-changing step. Motorized stage and maskless lithography system is used for the polymerization steps.....	5 9
Figure 3.9 Scanned image of 900 μm particles. Two hundred particles are fabricated with changing monomer only once. The particles are fabricated with the motorized stage.	5 9
Figure 3.10 Images of film combined glasses for high-throughput mask. lithography.....	6 1
Figure 3.11 Aligning process using microscopy images. Using the align key, the mask and glass substrate is aligned roughly, so the mask array and the polymer array is well paired. The colored magnetic monomer and transparent polymer can be distinguished well by microscopy images. Delicate alignment is performed to adjust location and angle of paired sets of the second mask and the firstly fabricated polymer.....	6 2
Figure 3.12 Microscope image of the firstly fabricated transparent polymer and the aligned set of the transparent polymer and the second mask.....	6 2
Figure 3.13 Scanned image of 900 μm particles. One thousand particles are fabricated with two times of sequential irradiation of patterned UV light through film combined mask glass. The particles are fabricated with film mask and parallel irradiation of UV light.	6 3
Figure 3.14 Silica coating process by the hydrolysis and the condensation of TEOS. The polymerized TMSPA is connected with the TEOS.....	6 5
Figure 3.15 Steps and functional groups for conjugating aminylated capture molecules to the silica surface of the encoded microparticles. Silanization is performed with APTES, and conjugation step is based on EDC / surfo-NHS reaction which	

guarantees chemical bonding which endures high temperature more than 100°C..... 6 7

Figure 3.16 Images of 900 μm encoded particles on different plates.

The particles are scanned in 400 dpi. Three images of particles except on 96-well plate show similar pixels for the area of the particles. The image of the particle on 96-well plate is blurred because the particle is located in the out of focus of the scanner. 7 0

Figure 3.17 Scanned images of 900 μm particles with various resolution.

For imaging 900 μm particles, the resolution of 1,200 dpi is selected as the most proper resolution in order to be decoded well and to use more than 100 pixels in analyzing colorimetric assay results [28]. 7 1

Figure 3.18 Algorithm of particle detection and decoding process.

The detected particles can be upside-down and rotated due to a random assembly of the encoded particles. To decode correctly with various codes like ‘đ, ƒ, π, ¼’ or ‘b, d, p, q,’ the particles should be appropriately oriented before character recognition process [28]. 7 2

Figure 3.19 Algorithm for adjusting flipped or rotated particles.

The center of an encoded microparticle is detected, and a line (yellow) is drawn toward the farthest edge of the particle. Two lines (red and orange) are drawn with the same angle to the edge from the center. The two lines are used to determine if the particles are flipped or not by comparing the length of two lines. Finally, the particles are oriented in a specific direction because the longest line (yellow) should be located in the left top [28]. 7 4

Figure 3.20 Image processing to read character codes in 900μm encoded particle.

The scanned images are changed in grayscale

images and then in binary images. After sharpening the images, the codes are read by the optical character reader.	7 6
Figure 3.21 Schematic of 300 μ m binary particles and spots for a region for colorimetric assay in center and eight regions for binary codes.	7 6
Figure 4.1 Schematic of immunoassay on encoded dual-function microparticle. The size of the particle is 900 μ m, and the particles are encoded with four lengths of character codes [28].	8 0
Figure 4.2 Plot and images to show the linear correlation between target concentration and color in scanned images. To check the color, median color intensity (MCI) is detected from the assay parts of the particles in scanned images of 1,200 dpi resolution. Rabbit anti-HisABP IgG is diluted in various concentrations using assay buffer. The results of the colorimetric assay were detected using anti-biotin gold nanoparticles and biotinylated goat anti-rabbit IgG which conjugate to encoded particles coupled with ANO2(1). MCI has an arbitrary unit, and error bars indicate \pm one intra-assay standard deviation [28].	8 2
Figure 4.3 Schematic of encoded particles and scanned image of particles with four different codes which was conjugated with four different antigens. The particles were incubated with pooled multiple sclerosis plasma samples. The samples were diluted 250 times with assay buffer. The image was obtained using an office scanner, and scanning resolution was 1,200 dpi [28].	8 5
Figure 4.4 Plot to show the difference between pooled multiple sclerosis samples and pooled health samples. To check the color, median color intensity (MCI) is detected from the assay parts of the particles in scanned images of 1,200 dpi resolution.	

The microparticles with four different codes were conjugated with four different antigens. The particles were incubated with pooled multiple sclerosis plasma samples or pooled healthy plasma controls. The samples were diluted 250 times with assay buffer. Error bars indicate \pm one inter-assay standard deviation [28]. 8 6

Figure 4.5 Median colorimetric intensity after performing 3-plex DNA detection from bacterial meningitis DNAs of 1 000 copies. Synthesized bacterial meningitis DNAs are diluted to have 1 000 copies in the solution. The particles are targeting sodC and lytA and negative control. 9 0

Figure 5.1 Comparable information and scoring of previously developed technology and colorimetric bead-based assay for multiplex point-of care detection [40], [47], [54], [67]–[74]..... 9 5

Figure 5.2 Positioning of colorimetric bead-based platform and other previous platforms. 9 5

Figure 5.3 Comparison of proposed platform with commercialized set-ups. Pros are noted in green and cons are noted in red, to be applied to multiplex high-throughput assay within a low-resource setting. The images are devices noted below respectively..... 9 7

Chapter 1. Introduction

In this chapter, a multiplex point of care test is described. The need for multiplex test and the unmet need of a decentralized multiplex point of care test is introduced sequentially. Finally, the idea of multiplex colorimetric assay platform with encoded microparticle is presented as the subject of this dissertation. This multiplex colorimetric assay platform uses a widely spread office scanner as a final detection tool of the multiplex colorimetric assay. The advantages of this scanner as a detector are explained compared to other imaging tools. The core technologies in the platform are dual-functional microparticle and signal enhancement from gold deposition on gold nanoparticles.

1.1. Multiplex point of care test

Multiple biomolecules in the blood can be used to identify physical or physiological states of people. Multiple molecules can identify the clinical status of a person more accurately and rapidly. Technology for screening multiple targets have been developed well. However, previously commercialized machines are limited to be applied to decentralized circumstance because they are reliable in high-resource laboratory settings. The decentralized multiplex screening is necessary to make higher social impacts to treat people in the world, especially with infectious diseases. The ideal multiplex point of care system should be informative and reliable to get enough information in clinical applications as well as cheap, automated and technically undemanding to be applied closer to the potential patients.

1.1.1. Multiplex assay for diagnosis of patients

A huge amount of information is integrated into blood [1], [2]. Blood includes biomolecules such as antibody, antigen, DNA, and RNA. These biomolecules are not only from the person but also the infectious bacteria, parasites, viruses or yeast if the person is infected. Specific targets in those massive amounts of biomolecules can be used to determine the physiological or pathological state of the person.

These biomolecules can be detected *in vitro* using capture molecules and detecting molecules [3]. Biomarkers are defined by the National Institutes of

Health (NIH) as “molecules that can be reliably and accurately measured and are indicators of normal or disease biological processes and responses to therapeutic interventions” [4]. The *in vitro* test can detect pathogens directly and rapidly from the blood, and there is no need for culturing in order to make accurate pathogen detection [5]. For typing and quantifying these biomolecules, the specificity of between antibody and antigen and between complementary sequences of DNA is widely used. Capture molecules are fixed on the specific region of the substrate to fix target molecules at the specific region. Detection molecules are combined to the target molecules at the specific region. Moreover, the detection molecules send an optical or electrical signal to quantify the amount of or typing the levels of the target biomarkers (Figure 1.1).

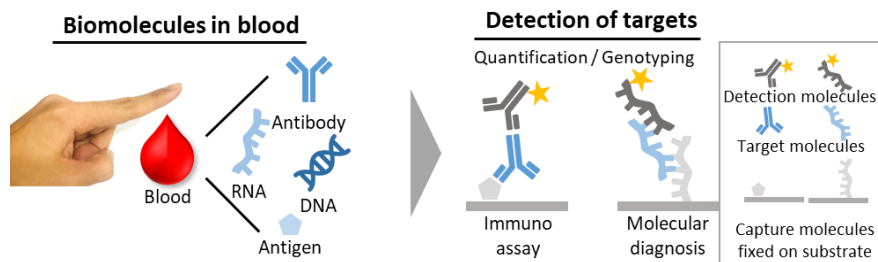


Figure 1.1 Detection process of target biomolecules in blood. Biomolecules include antibodies, antigens, RNAs and DNAs. The target molecules are detected with sequential biochemical reactions with capture molecules, target molecules and detection molecules. Target molecules can be quantified or typed with on-off detection.

These quantification or genotyping of specific biomolecules help to determine

a physiological or pathological state of a person in various diseases. For molecular diagnosis, laboratory polymerase chain reaction (PCR) test has been widely used with patients for clinical applications [6]. This research suggests that genotyping of biomarkers can affect clinical decisions. Besides, these accurate tests promote rapid therapeutic effect and reduce unnecessary sequential tests in the long term.

Multiplex assay helps to diagnose various pathological states of patients more accurately. In many instances, clinical information derived from a single target is not enough to diagnose or monitor diseases appropriately. Measuring multiple proteins and genes provides more accurate information for accurate and early detection in a personalized approach. For example, in diagnosing prostate cancer, multiple detections with five biomarkers have been shown to improve diagnostic accuracy to 99% from 70% with a single biomarker [7]. In detecting autoantibodies, multiple detections with three biomarkers allow to discriminate between celiac disease patients and healthy controls with raising sensitivity and specificity to 80%, which is not provided using a single biomarker [8]. In some cases, some specific biomarkers indicate the physiological state of a person so can be used to monitor the diseases of the person. Representative targets are elevated levels of low-density lipoprotein, cholesterol, and C-reactive protein which are related to cardiovascular disease [9]–[11].

With multiplex assay, it is easier to determine pathological states within similar symptoms of various infectious diseases. Many infectious diseases have similar signs and symptoms such as fever, headache, drowsy and muscle pain.

However, in today's real clinical tests, only standard and representative pathogens are tested which are associated with those symptoms. So many of infections are not diagnosed rapidly and accurately. Also, additional downstream tests are performed with extended time and inefficient treatments. Highly multiplex assay is used to help to provide a proper clinical decision accurately from various targets with many pathogen variations, compared to single-plex diagnosis [12]. In the process of diagnosis and monitoring, multiplexing is getting more critical. There are clinical needs to get more complex data to acquire accurate information because of the interplay between various and complex biological networks [13]. This rapid and accurate multiplex diagnosis also has economic profit with detecting antibodies [14] and genes [15]. Especially for infectious diseases, the rapid and accurate detection can decrease infection to healthy people from patients in which tremendous economic efforts are necessary.

The number of applicable biomarkers for multiplex tests is increasing in order to make multiplex assay more essential and useful. Biomarkers are detected continuously with simultaneous examinations of new analytes for various diseases. Advances in molecular biology, genomics and pharmaceuticals continue to discover an increasing number of applicable target biomarkers for diagnostic and therapeutic improvement [16]–[18].

1.1.2. Needs of multiplex point of care test near to patients

Although the multiplex assay has been developed for better treatment with the

rapid and accurate diagnosis, the social effect has not occurred in both high and low-income countries. That is because the experiments are held with well-developed laboratories with high resources including money and experimental settings [7]. Especially in low-income countries, the previously developed and commercialized systems are harder to be applied.

Decentralized multi-disease diagnostic platforms, which can simultaneously test for multiple infectious agents and pathogen variations, simplify disease diagnosis and management [19]. This multiplex point of care test (POCT) reduces the cost of testing, increases access to testing for poorly funded diseases, improves the management of coinfections and increases case-finding of individuals with specific coinfections [20]. So the decentralized POCT helps many situations including tests where a quick decision is necessary for decreasing number of patients of infectious disease. Moreover, there are so many cases where the patients do not return to the hospital for follow-up diagnosis and treatment although the diagnosis takes time. A sexually transmitted disease is a representative example where decentralized POCT can be effective [21].

Multiplex POCT is necessary especially for infectious diseases which are in veil (i.e. what, where and when the diseases emerge in the world). Emerging infections can be defined as “infections that have newly appeared in a population or have existed but are rapidly increasing in incidence or geographic range” [22]. These infections include respiratory infections, HIV/AIDS, diarrheal diseases, meningitis, influenza and others. Around 15 million global annual death is

estimated to have relation to infectious diseases in total 57 million death worldwide [23], [24]. There are many occasions of emerging and re-emerging infections (figure 1.2), and the regions of these appearances and spreads are not predictable as well as can be positioned where the high-resource settings are not prepared.

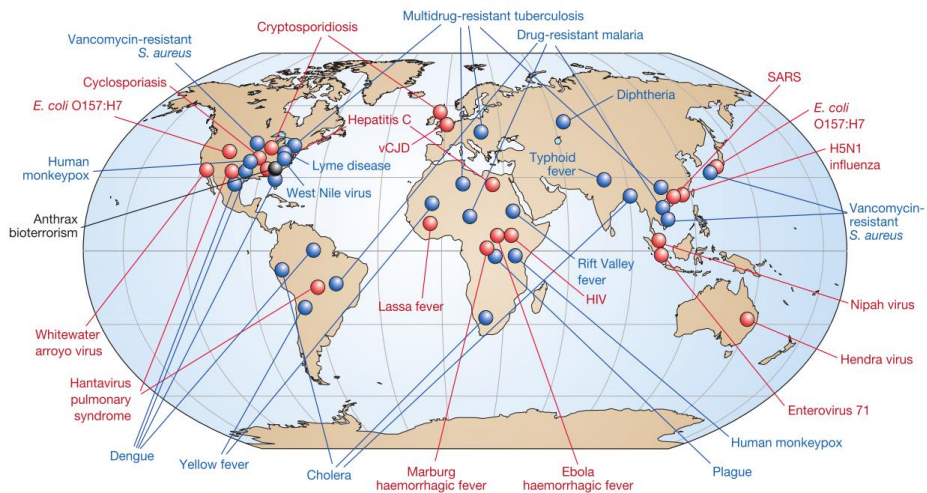


Figure 1.2 Schematic for indicating global locations where infectious diseases are emerged or re-emerged. Red dots indicate the locations where new diseases emerged, blue dots indicate the locations where diseases re-emerged or resurged and black dots indicate the locations where diseases emerge deliberately [23], [25].

Decentralized multiplex POCT helps to diagnose rapid and accurately within low-resource settings. For centralized multiplex tests, time delays are usually caused by sample transport to centralized laboratories and schedules in centralized laboratories with following low-plex tests. So the time to make clinical decisions can be shortened by switching conventional laboratory tests to decentralized

multiplex POCT. Diagnosis results from the multiplex data acquired at decentralized laboratories can be used to decide further testing or treatment.

The decentralized multiplex POCTs maximize the advantages with the availability of high-throughput tests. With a single multiplex test, the disease of a person can be diagnosed more accurately to be treated efficiently and decrease infections to healthy people. Rapid and accurate tests help physicians being able to access information faster and to treat more appropriately without unnecessary prescription [26], [27]. However, because of similar symptoms and active infections, it is essential to test enough amount of samples. So the multiplex POCTs have to be screened in high-throughput to maximize the impact in the case of infectious disease.

1.2. Main Concept: Multiplex colorimetric assay platform with encoded microparticle

The main objective of this dissertation is to propose and prove the concept of multiplex colorimetric assay platform using encoded microparticles (figure 1.3). This system has advantages in multiplexing capacity, decentralization of tests, and throughput of parallel tests. The multiplexing capacity is guaranteed with encoded microparticles with high capacity of encoding as labels to indicate target biomarkers fixed on the particles. The decentralization of tests is developed based on the technically and industrially low-resource setting. The assay results are detected with a widely spread office scanner by introducing colorimetric assay to

the multiplex bead-based assay. The parallel assays assure the throughput with the highly flexible bead-based assay system and the detection using office scanners where the broad field of view is guaranteed for the micro-sized particles.

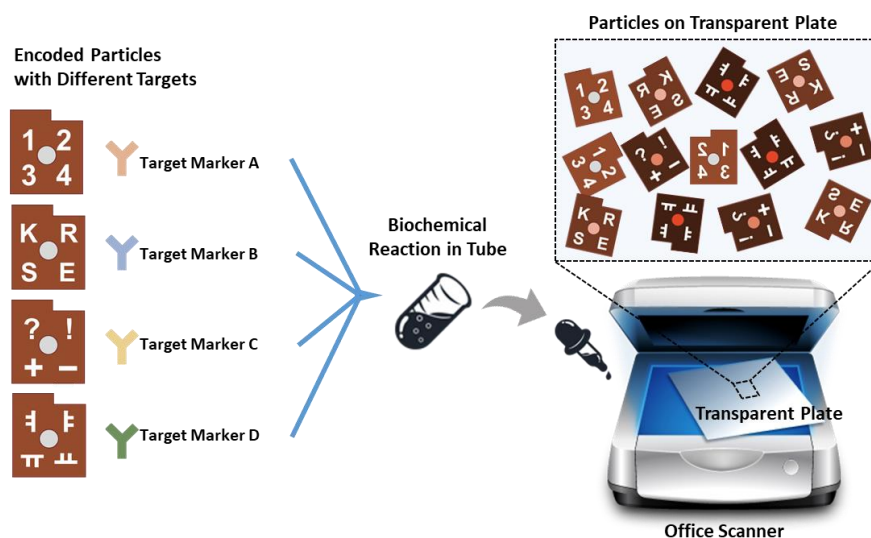


Figure 1.3 Schematic of system for scanner-based multiplex colorimetric assay with encoded microparticles. The encoded microparticles are conjugated with different targets via the codes. The encoded microparticles are pooled together and biochemically reacted in a tube with a sample including targets. Finally, the reacted particles are scanned on an office scanner [28].

1.2.1. Multiplex colorimetric assay platform with encoded microparticle

The multiplex colorimetric assay platform is described in this dissertation using encoded microparticles and scanner-based colorimetric assay with gold

nanoparticles. The encoded microparticles are conjugated with capture molecules which make specific binding of target biomarkers. The code indicates the type of the target molecules. After biochemical reaction in the tube, particles have the color change proportional to the amount of the target biomarkers. Samples are reacted in a separated tube with multiple encoded particles. The encoded particles are reacted and washed several times. Then, the particles are placed in the transparent plate on an office scanner. Finally, the particles are imaged by the scanner with showing code and color change (Figure 1.3). This detection with an office scanner is realized with the gold nanoparticles conjugated on the detecting molecules. The gold nanoparticles change the levels of target molecules into optical signals which can be detected by an office scanner. As a proof of concept to show that the platform can be applied to various targets, proteins and genes are detected in multiplex with this platform.

1.2.2. Advantages of scanner as widely spread detecting device

An office scanner has advantages as a low-resource setting because the scanner is cheap and already wide spread device. Compared to office scanners, the introduction of previous high-cost multiplex devices such as Ella® [29], Filmarray® [30], Verigene® and Luminex® [31] is costly in fixed cost to set up and requires a continuous variable cost because of expensive kit [32], [33]. This high cost is a big hurdle to introduce conventional devices to small decentralized faculties including small labs or hospitals.

Among the wide spread imaging devices including smartphones and cameras, the office scanner has advantages in imaging easily in high throughput (figure 1.4). The scanner has a large field of view with various options in resolution. Also, a scanner is free from focusing in order to image encoded particles compared to other devices like smartphones and cameras. Light exposure is stable because the light depends on the built-in light source of the scanner. Smartphone-based imaging can be affected by the external light under various circumstances [34].



Figure 1.4 Comparison between smartphone and office scanner. Smartphone system needs additional devices such as a lens and a focusing system. There are pros and cons of the devices. Pros are noted in blue and cons are noted in red.

1.2.3. Core technology of platform

In this platform codes and assay results of the multiple particles should be detectable by an office-scanner image. The codes of the particle indicate the target biomarkers and the color changes of the particle indicate the level of the target biomarkers. To realize scanner-based assays with high multiplexing capacity and high sensitivity, the encoded particles consist of two materials integrating a colored region showing the code and a transparent region having a low background color intensity to show colorimetric results with the high sensitivity. Additionally, a

signal enhancement strategy is introduced to this bead-based colorimetric assay by depositing gold molecules on the seed gold nanoparticles for detection.

One of the main difficulties of this platform is to show code and color change with limited imaging ability of an office scanner. Especially the codes should be detectable without any additional lens in which the boundary of transparent regions can be imaged in high quality. The color change, also, should be shown sensitively to achieve the meaningful limit of detection according to the target molecules. The scanned images cannot detect transparent particle well as the transparent particle has little difference with the background color. Compared to the microscopic images at high magnifications, the scanned images are limited to distinguish the regions with little difference in color. Furthermore, the scanned images cannot detect particle codes with groove form (figure 1.5) which have been developed to be applied to a highly multiplex platform with easily imaged by a microscope with lens [35]. For the colorimetric assay, the signal is weaker than that of the fluorescent assay. To achieve higher sensitivity, signal enhancement steps have been introduced to colorimetric assay using condensation of gold or silver to seed nanoparticles [36], [37]. Also, this system is applied to multiplex colorimetric assay [38]. However, this signal enhancement process has not been applied to bead-based assay in a multiplexing manner. It is because the deposition of gold on the encoded beads makes the codes of the particles disappeared. Especially the code as a thin groove on the particle is easily disappeared (figure 1.5).

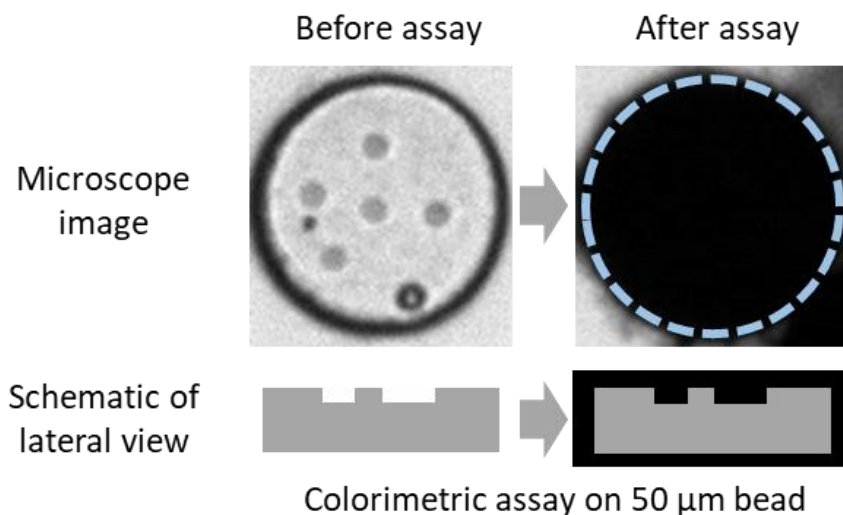


Figure 1.5 Microscope images and schematic of lateral view for before and after colorimetric assay with condensation of gold on 50 μm bead. The code of the particle is a groove form which is not holes. The condensation of gold is to enhance the optical color change in order to detect molecules with higher sensitivity. The condensation of gold inhibits code to be identified in bright field image from a microscope.

The strategies to overcome these main difficulties in this dissertation are using particles integrated with dual functions and introducing a signal enhancement step to the encoded dual particles.

The integrated dual functions are for higher sensitivity to detect biomarkers in colorimetric method and for detectable code which are achievable by RGB values of scanned images (Figure 1.6). To get the color change more sensitively, transparent particles have an advantage because transparent particles have no

background RGB value where the color change appears after colorimetric assay. Also, the RGB background value of particles have lower CV among the particles, which are fabricated in a different time with a newly prepared mixture of reagents. These low CV of transparent particles is more valid in a different circumstance of imaging from different scanners compared to the CV of already colored particles. Detectable codes on the particles are achieved with colored materials. The codes are not a groove form but a gaping porous form. With this gaping hole, the codes can be detected in high contrast with scanned images which integrate reflected light.

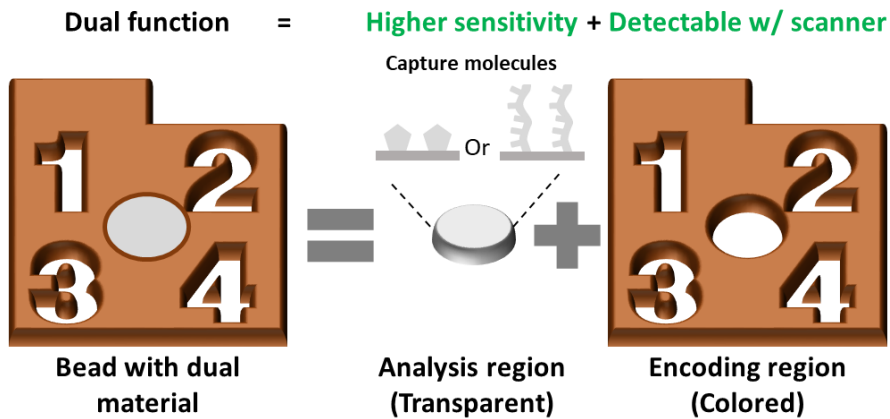


Figure 1.6 Schematic of particle consisting of dual functional materials. The particle is composed of two regions: an analysis region and an encoding region. Capture molecules are conjugated on all the regions but analyzing is performed with only on the transparent analysis region which has a weak color backgrounds. The encoding region is colored so easily detectable with scanning from office scanners without additional devices.

For higher sensitivity with a better limit of detection, the method for condensing gold to seed nanoparticles is introduced to the bead-based assay. Proportional to the levels of target biomarkers, the seed nanoparticles are connected on the surface of encoded particles. The seed nanoparticles show color change optically, especially in red value. However, this color change from the seed nanoparticles is weaker compared to the fluorescent change from fluorescent molecules which can be detected by fluorescent imaging. By an additional step of the condensation of gold, the size of the seed gold nanoparticles is increased, and

the enlarged gold particles reflect a lower amount light due to Plasmon resonances. So the particles after the condensation step have higher RGB value in scanned image (figure 1.7). This signal enhancement step makes sensitivity of tracking the level of target biomarkers higher, namely the limit of detection lower. This enhancement of colorimetric signal has similar sensitivity compared to fluorescent detection [36].

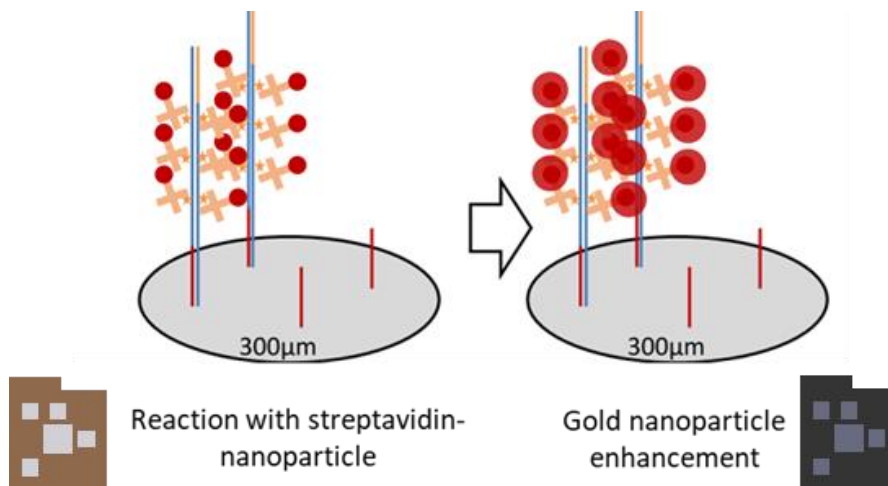


Figure 1.7 Schematic of signal enhancement step using condensation of gold around the seed nanoparticles conjugated to the surface of the encoded particles. The seed nanoparticles are conjugated on the encoded microparticles after colorimetric assay, but the visible color change is not enough to be imaged by an office scanner. With a signal enhancement step using gold condensation, the visible color of encoded microparticles changes more dramatically to be detected by the scanned images.

1.3. Outline of dissertation

In this dissertation, a new concept of multiplex bead-based colorimetric platform is proposed and explained. In Chapter 2, the previous methods and commercialized multiplex POCT platforms are described and compared in an aspect of technical background, multiplexing capacity, throughput, and cost. Then, previous research of my group is explained. In Chapter 3, development and optimization process of the platform is described. The process is described sequentially: preparing encoded particles for colorimetric assay, performing massively parallel multiplex colorimetric assay, optimizing imaging process with an office scanner, and analyzing scanned images. In Chapter 4, antibody detection and gene detection with this platform are described sequentially, as a proof of concept to be applied multiplex assay with various kinds of targets. Finally, in Chapter 5, there are discussions about the proposed platform. The summary of the dissertation is noted with a comparison with previous technology, the limit of the platform and future work.

Chapter 2. Background

In this chapter, previous studies for the multiplex assay to detect biomarkers from the blood of patients. The conventional method to detect biomarkers and the commercialized point-of-care devices are covered. In addition to the description, the comparison of previous studies is described in the aspect of multiplexing capacity, throughput, and cost. Finally, the previous related research in my group is described.

2.1. Process of multiplex assay

The multiplex assay is detecting multiple biomarkers in a single sample at the same time [3], [35], [39]. In the process of detecting biomarkers, target molecules are captured by capture molecules which are confined in the specific region on purpose of labeling. The confined capture molecules help to fix specific target biomarkers on the confined specific regions, and the detecting molecules change the level of target biomarkers into the electrochemical or optical signals which can be easily detected by proper detecting devices. To detect multiple biomarkers simultaneously, various capture molecules are positioned and confined on the specific region to label target markers with the same signaling method to be detected. The intended fixing regions indicate the type of target biomolecules. Then, various capture molecules and the various target biomarkers are reacted simultaneously with a single sample in a separated chamber. Parallel assay with various samples can be performed not in a single chamber but separated multiple chambers. The specific binding of biomolecules guarantees the specificity between a capture molecule and a target biomarker. For example, monoclonal antibody reacts specifically to a target antigen without cross-reactions, and single-strand DNAs specifically bind to single-strand DNAs with complementary sequences. For multiplex assay platforms, the unspecific binding should be prevented. Namely, the reactions from the specific binding of molecules should be guaranteed as only one

reason to make detecting signals. Unreacted residues including unreacted reagents in the sample are washed out. Then, the detection molecules bind globally to a complex of capture molecules and target molecules. The detection molecules take a role to generate electrical or optical signals proportional to the level of target molecules.

2.2. Previous multiplex point of care technology

For the multiplex assay, essential criteria are the amount and the quality of information from a sample in a small volume with easily accessible process [40]. For the rapid test with reliable quantification, multiplexing capacity and high sensitivity are vital for the platform. For multiplex POCT, accessibility of the platform is important in addition to the amount and the quality of information derived from the small volume of the sample. High accessibility is derived from low-resource setting and operation-free steps to be performed efficiently in a short period by non-experts. The low-resource setting is essential to make the platform to be used closer to the patients. Because the high-resource setting is a big hurdle to set up and start experiments with the platform. Especially for decentralized faculties such as small laboratories or hospitals, low-resource is more critical.

Multiplexing can be realized through spatial separation or different labeling of capture molecules. To date, spatial separation of various capture molecules is widely used with printing technology. In paper-based assay and array-based assay, capture molecules are spatially separated and fixed on the specific surface of a

plate. Multiple biomolecules react at the specific position via targets. So the position of reaction results show the types of capture molecules. In a microfluidic-based assay, capture molecules are separated in a different chamber such as well or droplet. Labeling technology is usually used for the bead-based assay. The beads can be labeled by fluorescence [41], [42], color [43], or shape [44]–[46]. Capture molecules are fixed on the beads so multiple components can react at once. This bead-based assay is also called as a suspension assay because labeled beads are suspended free in the reaction chamber which promotes reactions among the capture molecules, target molecules and detecting molecules.

2.2.1. Technology for multiplex point of care test technology

For multiplex point of care assay, a highly informative and accessible technique has advantages. Many methods have been proposed and developed with using various technologies. Spatial separation using spotting capture molecules in an array format has been the most often applied method. This technique is widely used with high accessibility in the paper-based assay. Also, with microarray technology, highly multiplex assay has been performed in the laboratories. However, this technique is highly accessible only with low multiplexing capacity and complex because of device fabrication, assay preparation, and signal readout, especially in higher multiplexed targets. Microfluidic technology, also, has been introduced with the strength of separating liquid in a small volume. However, the microfluidic-based system is hard to improve multiplexing levels in the aspect of

increasing variety of targets, although this platform is easy to increase multiplexing level with diluting same targets. Another technique used frequently for the multiplex assay is bead-based technology with labeling technique. This bead-based technique has strength in multiplexing capacity and higher sensitivity due to suspension assay. However, the bead-based assay is complex in imaging and data-analyzing process to detect and decode the label of the beads.

Paper-based assay [47]–[50] is highly accessible due to operation-free process and instrument-free detection with on-site lateral flow assay (figure 2.1). For example, pregnancy test kits are one of the best-established products where the tests are simple, fast and low-cost. However, the paper-based assay has limited flexibility in designing assay and low sensitivity compared to other methods. Especially, increasing the multiplexing capacity is limited because of the printing process in the device preparation step. Besides, the operation-free paper-based assay has low sensitivity which makes the platform applied to limited targets which are plenty in a sample. Signal enhancement steps have been applied to the paper-based assay to achieve higher sensitivity, but the advantage of high accessibility is weakened because of additional signal enhancement steps and imaging process with the high-resource setting. With high accessibility, 3-plex [51] and 5-plex [47] assay has been proposed.

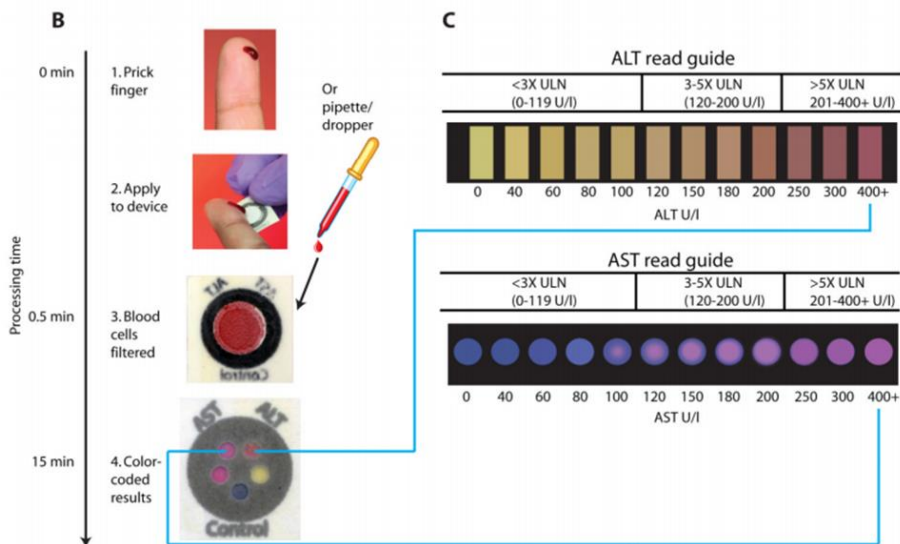


Figure 2.1 Schematic of design and protocol of paper-based test from blood. The device is operation-free in the multiplex assay from a drop of human blood. This paper has five detection zones, and each target is quantified by color in each zone. The paper consists of two layers of papers. One is a plasma separation membrane, and the other is a laminated cover of a polyester film where patterned hydrophobic channels are integrated. A drop of whole blood which is around $30 \mu\text{l}$ is necessary for quantification of multiple targets. In the plasma separation membrane, blood cells are filtered out, so only plasma can pass through. The test takes around 15 minutes, and the results are matched through the color guide. [47].

Array-based technique realizes highly multiplex assay due to well-developed microarray technology [52]. The microarray is not proper to highly accessible point-of-care tests because microarray printing in high-throughput takes a long time and the high cost. The high-resource setting is, also, necessary for imaging

microarray.

Microfluidic technology has been introduced to the multiplex assay with the property of the platform without complicated, laborious operations (figure 2.2). The microfluidic technology has been developed to integrate large scale assay in the small chip [53]. Microfluidic technologies integrate various biochemical reactions for immunoassay and genotyping and sequential or parallel procedures into a miniaturized chip in which fluids are manipulated within small volume [54], [55]. Multiple analytes can be detected within small microfluidic devices [56], [57]. The power source of the microfluidic platform can be physical force from pressure, capillary or centrifugal force. The microfluidic platform using centrifugal force is named lab-on-a-disc platform (figure 2.3). The reagents flow or not depending on the speed of the rotation.

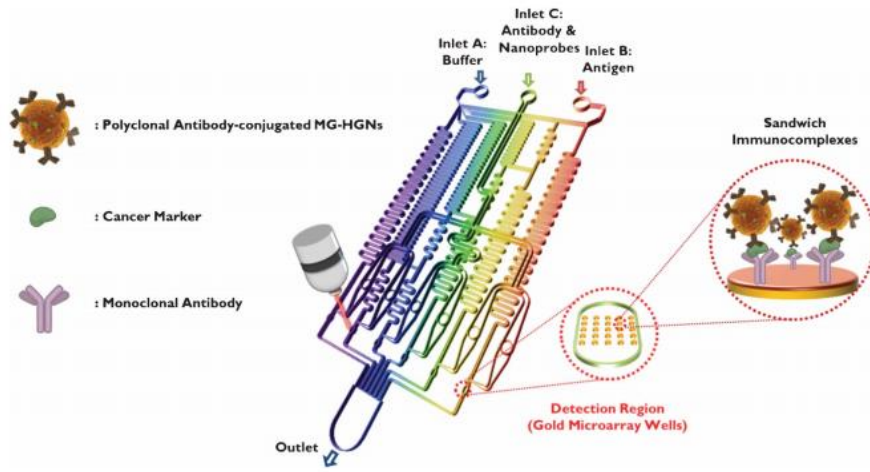


Figure 2.2 Schematic of a microfluidic platform which integrates sequential and parallel steps for detecting multiple analytes [58].

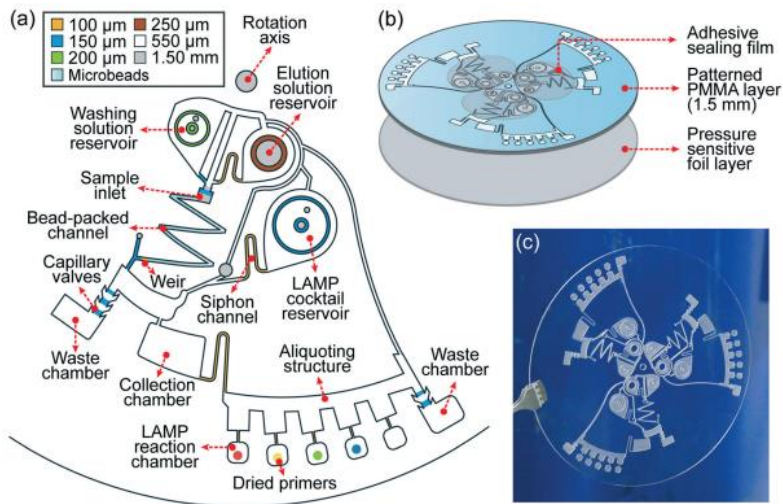


Figure 2.3 Design of lab-on-a-disc which includes various steps for detecting target biomarkers. Centrifugal force works as a power source of fluid and a valve controller [59].

Bead-based technology allows measuring the level of multiple biomarkers simultaneously in high throughput from a small volume of a single sample. The beads are labelled by optically or electrically to identify conjugated capture molecules (figure 2.4). With these labels, multiple biomolecules can be detected simultaneously [60]. Luminex beads are one of the most widely used for bead-based assay with having multiplexing capacity up to 500 with differently encapsulated fluorescent molecules [31]. Luminex beads are encoded by the various degree of fluorescent intensity. The high multiplexing capacity is the strength of the bead-based assay, so the encoding capacity of bead has been studied to achieve high multiplexing capacity with various kinds of codes including fluorescence, color, shape, and others [42], [61], [35], [62]. Another fluorescent signal finally conjugated detecting molecules shows the level of target analytes [63]. The bead-based assay is a kind of suspension assay in which molecules freely float in the solution. The free-floating promotes the reaction between the molecules so that higher sensitivity can be achieved. The fluorescence of beads in two different kinds of emission wavelength can be detected in fluorescent flow cytometry (figure 2.5 (a), (c)) [64], [65]. With integrating magnetic property to the fluorescent beads, the fluorescent signal can be imaged by a camera without flow cytometry. The magnetic force is used to assemble magnetic fluorescent beads in a single layer right before imaging. The beads are fixed at specific positions without moving while imaging in two kinds of fluorescence with different wavelengths (figure 2.5 (b), (d)).

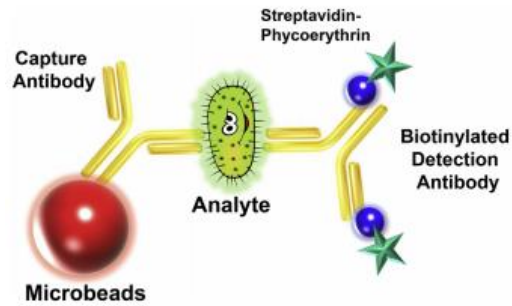


Figure 2.4 Basic principles of bead-based immunoassay for multiplex colorimetric assay. The microbeads have a different degree of fluorescence as a label for the capture antibody. The tagged detection antibody indicates the existence of the analyte connected to the microbeads [66].

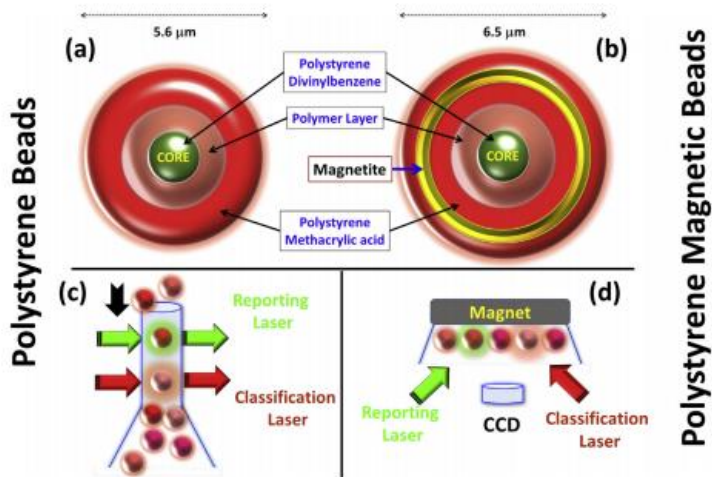


Figure 2.5 Type and detecting process of microbeads conjugated with target biomarkers for multiplex assays. Code and level of biomarker are detected in a fluorescent flow cytometer approach or fluorescent imaging approach after assembled in a single layer by magnetic power [66].

2.2.2. Positioning of previous technology for multiplex assay

For multiplex point of care assay, a highly informative and accessible technique has advantages. Each technology for multiplex POCT has advantages and disadvantages because all the criteria cannot be fulfilled because of the correlation between better information and better accessibility. So the previous technology is positioned for different properties in these criteria with targeting different applications or situations in which the merit of the technology is maximized (figure 2.6, table 2.1).

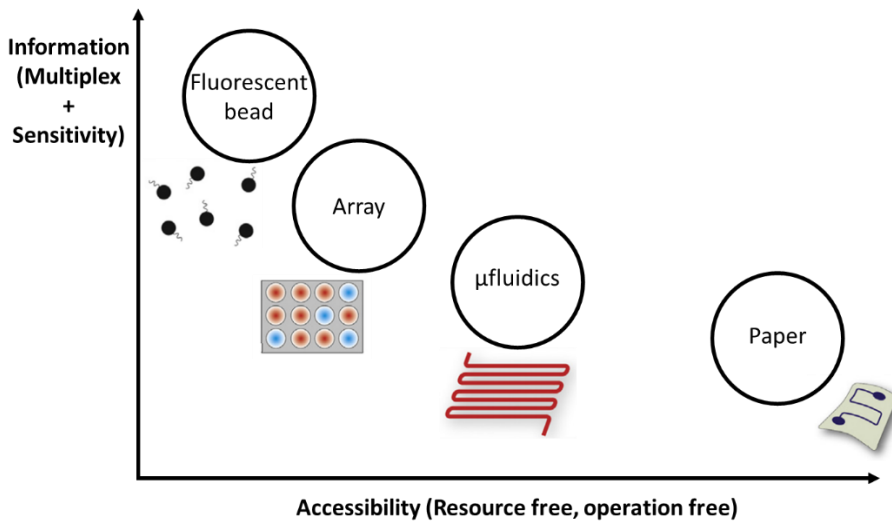


Figure 2.6 Positioning of conventional technology for multiplex POCT. The accessibility of the platform and the information derived from the platform are considered critically. The axis of accessibility counts how high resources and how much operations are necessary. The axis of information counts the multiplexing capacity and the sensitivity [40].

Table 2.1 Comparison between previously developed technologies [40], [47], [54], [67]–[74]. Representative properties are noted because each technique has edited versions where the characteristics are different with compensation between the topics according to applications.

Topic	Fluorescent bead	Paper	Array	Microfluidic
Multiplex	50 – 500, Extendable	1 - 5	10 – 10M, Extendable	2, 5, 8
Sensitivity	Very high	Low	Very high	High
Resource setting	Fluorescence, Flow cytometry	Eye, Phone, Scanner	Electrical or optical device, Array setup	Eye, Phone, Scanner
Operation	Highly necessary	Free	Highly necessary	Necessary

Although the previous technique has not been achieved as a highly informative and accessible platform, each technique has been developed well and widely used in specific applications in which the advantages of the technique are maximized. However, there are still unmet slots for specific situations in which informative assay is necessary within the low-resource setting (figure 2.6).

2.3. Commercialized multiplex assay devices for point of care test

Many companies have developed commercialized multiplex assay machines [40], [75]–[77]. Many types of technologies are integrated into the commercialized

machines including microfluidic, array-based and bead-based technique. Representative machines are Ella® for immunoassay and Verigene® and Filmarray® for genotyping. These machines integrate many sequential processes such as preparation, extraction, amplification, capture, washing, and detection. Also, the company Luminex has many automated imaging machines which integrate many steps but only in the process of imaging. Flexmap 3D®, Luminex® 100/200 and Magpix® are automated detection machines in which input should be the products from the reaction between kits and prepared samples.

Ella® of Proteinsimple is automated immunoassay machine using microfluidic technology (figure 2.7) [29]. Reagents for capturing and detecting target biomarkers are prepared at specific areas in the microfluidic channel. After loading a sample to perform a multiplex assay, the reactions with reagents are performed sequentially in the microfluidic channel. The reactions with different targets are performed in geographically separated chambers, so the platform is free from cross-reaction. The sequential reactions without pipetting and the geographical separation can be achieved with a valve system integrated into the microfluidic channel. This machine is using serum samples. The serum samples should be extracted from blood with a kit and centrifuge.

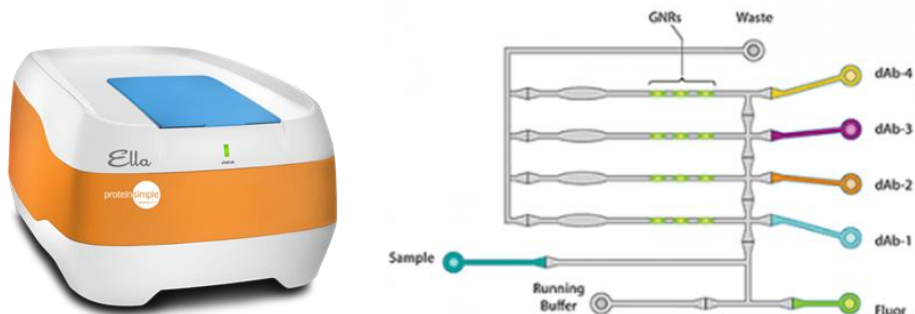
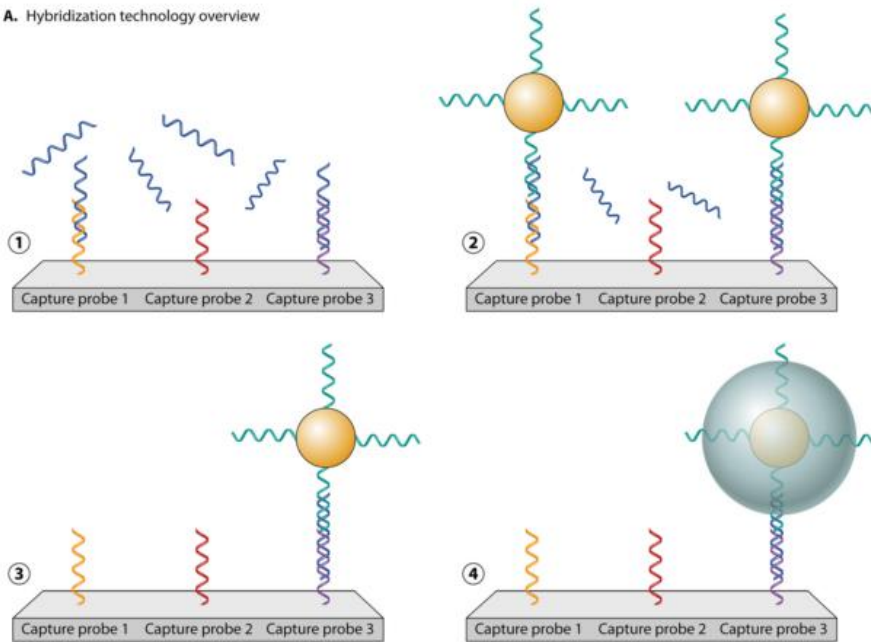


Figure 2.7 Image of Ella® and schematic to show principle of Ella®. The Ella system uses the microfluidic system and detects multiple analytes in separated chambers. The valves are used to perform sequential reactions in the microfluidic channel. The final signal is detected in fluorescence.

Verigene® of Luminex is a fully automated genotyping machine using microfluidic, bead-based and microarray-based technique (figure 2.8) [31], [78]. The primary technique applied to this platform for detecting multiplex biomarkers is a microarray-based technique. Two machines have been developed with different functions for multiplex assay. One is Verigene Processor for automated assay process, and the other is Verigene Reader for imaging and analyzing reacted components. This machine can be reacted with blood samples because the machine is fully integrated with various functions including PCR and signal enhancement. This machine has been proven to show similar quality compared to previously widely used Luminex beads [79], [80]. Gold nanoparticles with capture DNAs react with the target biomarkers in the sample. The nanoparticles conjugated with target molecules are reacted with the microarray. In the microarray target-specific

capture DNAs are spotted on the specific region of the microarray. The target regions of the gold nanoparticles and the target regions of the microarray are different. So the gold nanoparticles bound to specific target molecules are positioned on the specific regions for the specific target molecules. The gold nanoparticle is coated with silver to increase optical signals to indicate levels of target molecules. The microarray is scanned in the Verigene reader with the enhanced optical signal. The reader calculates the optical signal and matches with the position which indicates the types of the target molecules. The reagent kit for this platform is named as a cassette which contains hybridization reagents, fluidic system, and microarray.

A. Hybridization technology overview



B. Example array design

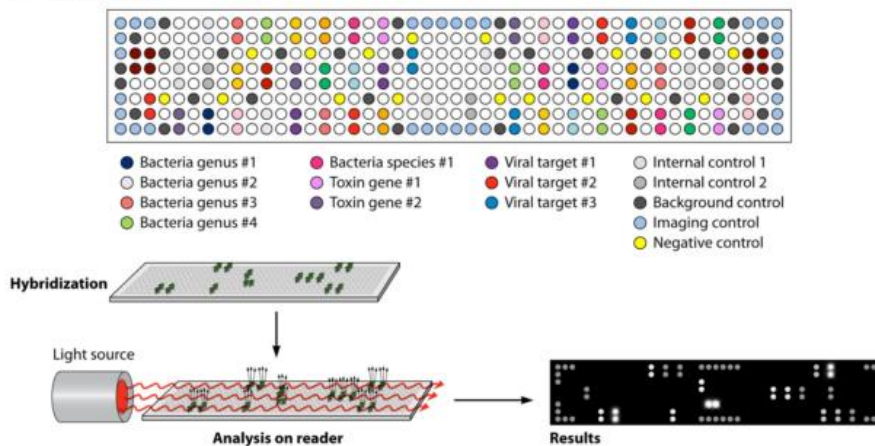


Figure 2.8 Schematic of principle for Verigene® solid-phase microarray. The targets are conjugated with two types of components which are conjugated with target-specific capture molecules. The single-stranded capture molecules are immobilized on the specific position of microarray and particles. (A) The position

of capture molecules in microarray indicates the targeting probes. The target probes are annealed to the complementary capture probes on the microarray. Other capture molecules which are targeting different regions of target molecules are conjugated to gold particles. So the gold nanospheres can be immobilized on the specific region of the microarray glass by annealing to the complementary targets. The whole chip is washed to remove unbound residues such as genes and gold particles. By condensation of metal materials, the optical sensitivity increases for detection with higher sensitivity. (B) Target-specific capture molecules are aligned and conjugated on the specific regions on purpose. Each kind of capture molecules is positioned in three different regions to be tested in triplicate for higher accuracy of results to be guaranteed. (C) Targets are detected in bright field images. A light source irradiates light across the array. Then, the optical camera can image the regions in a bright field with colorimetric results [77].

Filmarray® of Biomerieux is, also, a fully automated genotyping machine using capillary-based fluidic and array-based technique (figure 2.9) [30]. Filmarray® is integrated with functions for physical lysis, two times of sequential PCRs and fluorescent imaging. Cells in the blood including viruses, bacteria, yeast, and parasites are lysed chemically and physically at the first chamber. So the target genes are extracted and prepared for the reactions. Then the multiplex PCR is performed for 27 cycles in the second chamber. Finally, the products of the first multiplex PCR are diluted in 100 times and then separated to the regionally separated chambers. In each separated chamber, a different set of forward and reverse primers are pre-loaded and the second stage PCR is performed for 30

cycles. Finally, fluorescent molecules targeting double strand DNAs which exist only in the chamber with amplified DNAs with proper targets and primer sets. The fluorescent image shows the levels of the targets and the types of target analytes can be recognized by the position because the primer sets are loaded to the intended specific region. The reagents for the assay is pre-loaded in the film and freeze-drying technology helps the storage of the reagents.

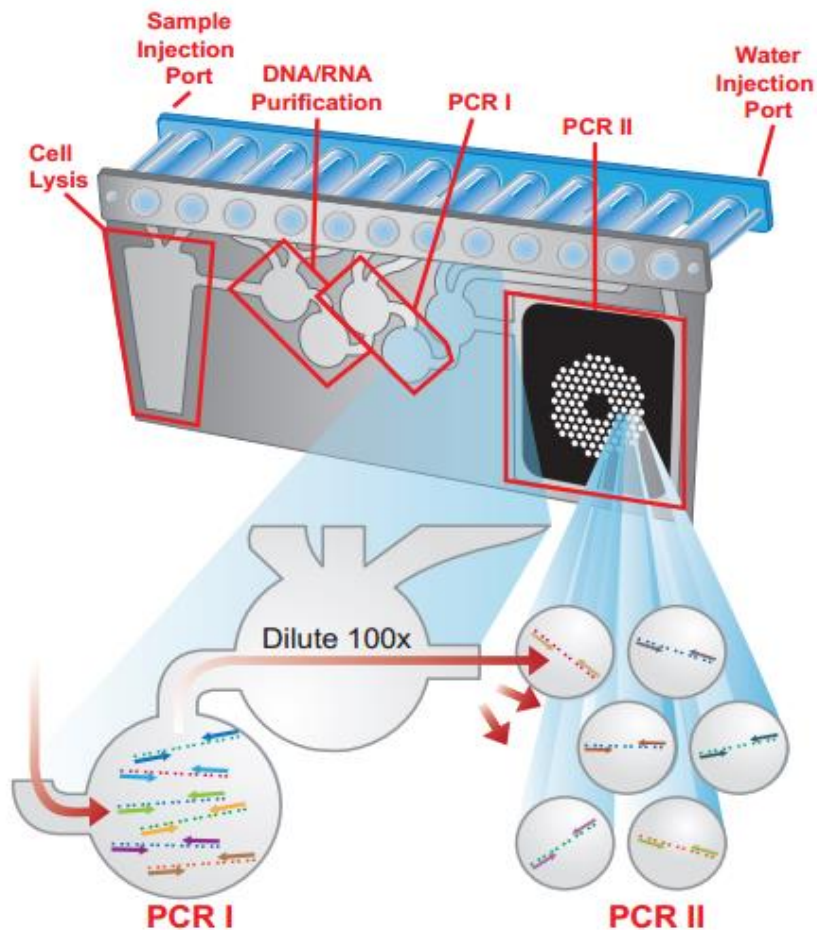


Figure 2.9 Schematic of cartridge and principle used in the Filmarray® device.

Physical lysis is performed in the first chamber to analyze various cells in blood including viruses, bacteria, yeast, and parasites. Then two-stage PCR is performed. The first PCR is multiplex PCR and the second PCR is a single set of PCR in separated microwells. Then, final results are imaged with fluorescent signals targeting secondly amplified DNAs [30].

The company Luminex has automated detection machines for the bead-based assay (figure 2.4, 2.5) [31]. These machines are Flexmap 3D®, Luminex® 100/200 and Magpix®. These systems are not automated for preparation of the sample, amplification of target markers, and sequential reactions between fluorescent bead kits and samples. The fluorescent beads after reaction have two kinds of fluorescent signal. One is for labeling of target biomarkers, and the other is for indicating the levels of the target biomarkers. Flexmap 3D® and Luminex® 100/200 detect fluorescent signals with fluorescent detection through flow cytometry (figure 2.5 (a), (c)) and Magpix® detects fluorescent signals after assembling beads on the well using magnetic force (figure 2.5 (b), (d)).

2.3.1. Pros and cons of conventional automated machines for multiplex point of care test

The conventional machines are developed for specific situations and applications but to be used for ideal multiplex POCTs, the machines have limits such as multiplexing capacity, throughput to test a number of patients and needs of high-resource setting with a high cost.

Ella®, Verigene®, and Filmarray® are representative machines among the fully automated multiplex assay machines at relatively low prices. More expensive machines are for different applications which need high-resource laboratory settings in which higher ability is necessary with higher prices. Ella® is for detecting proteins, and Verigene® and Filmarray® is for detecting genes. These machines are fully automated to test from the proper format of the samples to final analyzing results of multiplex assays. Moreover, Verigene® and Filmarray® do not need a long preparation step. Just mix patient blood and kit and insert them in the machines. Ella® should extract serum from patient blood to test. However, serum extraction can be done without difficulty using a centrifuge. Running time is short for the devices. It takes around 1 to 2 hours to get results from the samples. These machines are developed well to make full steps operation-free and fast with short hands-on time.

Many clinical diagnostic applications require not only automated simple operation but also inexpensive assays which can be done without expensive additional devices. However, these devices are quite expensive per machine. The price of a single device is around \$40 000 - \$90 000. And the prices of kits are expensive to compensate the low-profit-margin. The prices of kits are around \$80 - \$250 for testing a sample.

Table 2.2 Characteristics of automated multiplex assay devices with commercialization [29]–[32], [77].

Topic	ELLA®	VERIGENE®	FILMARRAY®
Multiplexing capacity	4	9-16 (Extendable to 400)	14-27 (Extendable to 100)
Target	Protein	Gene	Gene
Core technology for detection	Microfluidics	Microarray	Microarray
Throughput per run	16, 32	1	1
Price of device	\$90 000	\$40 000	\$60 000
Price of kit	\$150-\$250	\$80-\$160	\$155
Run time	1.5 hours	1-2 hours	1 hour
Hands-on time	15 minutes	5 minutes	2 minutes

Ella® is a representative system for multiplex immunoassay. This machine is technically based on microfluidics. This machines can analyze up to 32 samples in a single assay. However, the multiplexing capacity is low. Targets can be analyzed simultaneously up to 4 analytes. The final results are detected in the separated chambers so this platform is freer from cross-reactions compared to other platforms. Also, the limit of detection and the dynamic range are good as several pg/ml and 4-5 log, respectively. The sample volume is also reasonable from 2.5 μ l to 25 μ l

serum.

Table 2.3 Information of conventionally developed machine for multiplex POCT of protein [29].

Machine	Multiplex	Run time	Hands-on time	Dynamic range	Limit of detection	Throughput per run	Sample volume
ELLA®	4	1.5 hour	15 minutes	4-5 log	pg/ml	16, 32	2.5-25 µl

Verigene® and Filmarray® are for multiplex genotyping with high multiplex capabilities compared to other devices [77]. These machines have a quite a high multiplexing capacity because these machines use microarray format for final detection. The commercialized kits are up to 16 and 27 respectively, but the microarrays of these machines can cover up to 400 and 100 targets respectively. Nevertheless, the throughput of a single machine is extremely low, so these devices have low scalability. A single machine of two types of devices can analyze one sample per 1-2 hours. To scale up the throughput to test 100 patients per day, with fully operating machines during 8-16 hours, 12 machines are necessary and it costs \$260 000 for Verigene® and \$720 000 for Filmarray®. To scale up to test 1 000 patients per day, 125 machines are necessary and it costs \$2 600 000 and \$7 500 000 respectively. This high cost for high-throughput tests limits the device to be utilized at quite centralized centers, although it is fully automated machines for highly multiplex genotyping with realizing fast and operation-free detection.

Table 2.4 Estimated prices of Verigene® and Filmarray® with considering maximum throughput per day [30], [31].

Topic	VERIGENE®	FILMARRAY®
Target	Genes with fixed panel	Genes with fixed panel
For 100 patients per day	12 machines are necessary (Instrument: \$260,000)	12 machines are necessary (Instrument: \$720,000)
For 1,000 patients per day	125 machines are necessary (Instrument: \$2,600,000)	125 machines are necessary (Instrument: \$7,500,000)

Luminex bead systems have been developed with high multiplexing capacity and high flexibility. Although this system is not free from operations, this platform is highly flexible to change the number and the types of targets for multiplex assay as well as the throughput with parallel assays. These Luminex bead systems are using the fluorescent bead-based technique. These beads are fluorescently encoded and the levels of the multiple targets are shown in fluorescent signals. Various machines have been developed to detect codes and signals with a different spec and named as FLEXMAP 3D®, Luminex® 100/200™ and MAGPIX® (figure 2.10). These platforms have different specs in multiplexing capacity, the structure of beads and imaging methods. FLEXMAP 3D® and Luminex® are integrated with fluorescent cytometry and MAGPIX® is integrated with fluorescent camera imaging and assembly system using magnetic force. The price of machines and kits are expensive similar to automated conventional machines. It is because the system

needs to compensate the cost for high-resource settings.

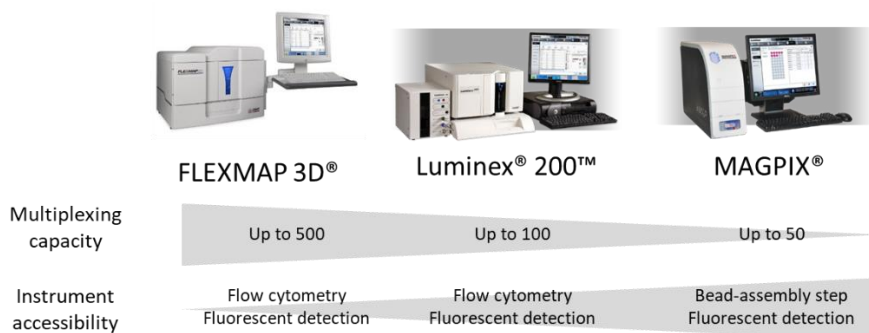


Figure 2.10 Images and spec of commercialized Luminex devices for fluorescent bead-based assay. The devices have different methods for imaging, and the multiplexing capacity differs by the type of machines [31].

2.4. Previous research in the group

My group has proposed shape-encoded microparticle system for the multiplex assay (figure 2.11) [35]. The platform is similar to the Luminex bead system in multiplexing capacity and assay process for detecting the level of targets in a multiplexing manner, but the encoding method is different. The particles are encoded with shape codes (figure 2.11(b)). Compared to Luminex bead, the shape-encoded microparticles can be decoded with bright field images without flow cytometry nor fluorescent detection. Also, the particles are flat so that this shape codes can be easily scanned with the bright field images. However, this shape-encoded microparticle system, also, relied on fluorescence imaging to detect the level of target molecules. So fluorescent imaging tools are necessary. For example,

in this experiment, fluorescent microscopy is used to get images for genotyping.

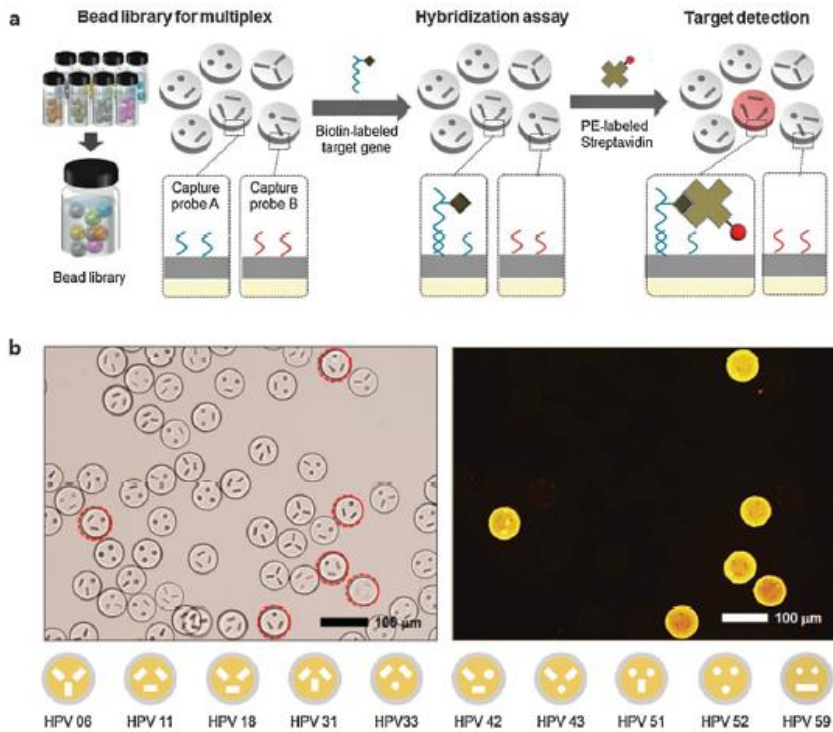


Figure 2.11 Schematic and images of multiplex HPV genotyping performed using encoded and silica-coated microparticles with shape codes. (a) A schematic explaining the process and principle of multiplex HPV genotyping using encoded silica-coated microparticles and streptavidin which is chemically conjugated with fluorescent molecules. Silica-coated microparticles are suitable for inhibiting unspecific binding to the particles. (b) A bright-field and a fluorescence microscopy image are shown after the assay for genotyping. The shape codes can be read within a bright-field image, but assay results should be read using a fluorescent image. In the fluorescent image, the particles with probes complementary to the target HPV 33 sequences show strong fluorescence. It is because only HPV 33

targets are used for the assay and it shows the availability of the platform as a genotyping tool [35].

Chapter 3. Platform development

In this chapter, the entire process is described for developing scanner-based multiplex assay platform with encoded microparticles (figure 3.1). The process starts with preparing encoded microparticles conjugated with capture molecules. Dual-functional particles are fabricated to have colored shape codes which can be detected well by a scanner and transparent region to show the change of color by the assay sensitively. Then, a massively parallel multiplex colorimetric assay is performed using the prepared particles and gold nanoparticles to change the level of target biomarkers into an optical signal in a bright field. Finally, the encoded particles after colorimetric assay process are imaged by a scanner and the image is analyzed for decoding the codes of the particles indicating the target biomarkers and analyzing the levels of biomarkers.

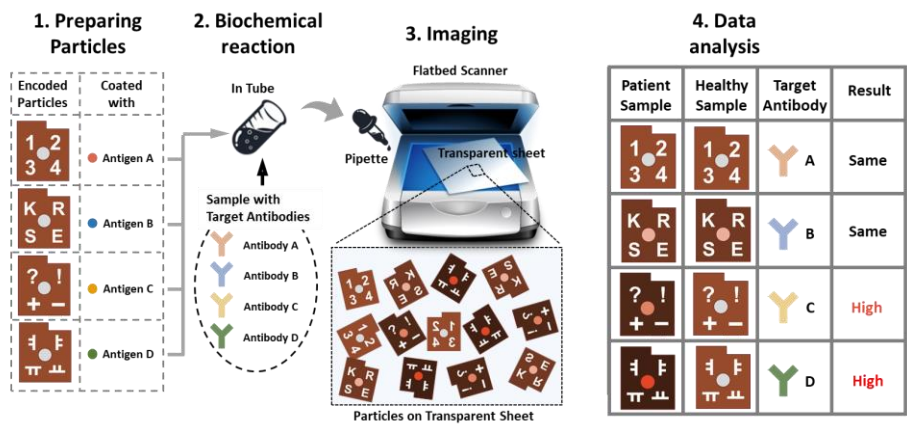


Figure 3.1 Schematic of the developing process of the scanner-based multiplex colorimetric assay platform. The process is preparing particles, performing the biochemical reaction, imaging with an office scanner and analyzing data from the image [28].

3.1. Preparing process of encoded microparticle conjugated with capture molecule

The colorimetric multiplex assay starts with preparing dual-functional encoded microparticles which are conjugated with capture molecules. The primary functions of the particles are codes to identify target molecules and the ability to show color change to estimate levels of target molecules. These two main functions should be recognized by the scanned image of widely spread office scanners.

In the process of designing particles, imaging circumstance of office scanners should be considered. So the design considerations include making particles have dual functions for colorimetric assay on the beads and keep dual functions in the

scanned resolution of office scanners. Multiplexing capacity is also an important factor for designing particles.

With the proper design of particles, the dual-functional encoded particles should be fabricated. To make particles, the photolithography technique is used. With patterned UV light, monomers with photoinitiators are polymerized in the shape regarding the pattern of UV light. For making dual-functional particles, two materials are polymerized sequentially.

To fabricate sequentially with two materials and, at the same time, make the two materials are integrated as a dual-functional single particle, the strategy is to fix the firstly fabricated particles at the specific position of the substrate. With this fixation, the firstly fabricated particles can be located at the same position after washing and changing monomer for the second fabrication. The substrate should be aligned at the same position where the first fabrication is performed.

To guarantee the platform to be prepared easily for high-throughput assay, the high-throughput fabrication method is studied with mask lithography. With this mask lithography, the particles can be prepared enough in a high-throughput manner.

The fabricated particles are conjugated with capture molecules in massively parallel. The particles are coated with silica to inhibit unspecific binding to particles. Then, the functional groups on the surface of the silica coating are changed to carboxyl groups. Finally, the carboxyl groups are chemically conjugated with amine groups of the capture molecules.

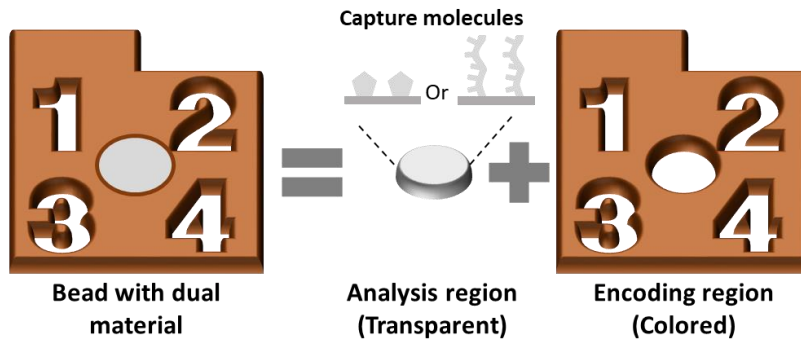
3.1.1. Particle design considerations for scanner-based detection

For multiplex colorimetric assay platform, the particle should have two functions. One is to indicate target molecules, and the other is to represent the level of target molecules. As a decentralized platform, the code and the representation of the target levels should be imaged stably by office scanners.

To make platform have high multiplexing capacity, shape code is selected. There are many methods to encode particles including fluorescence [42], color [43], [81], size [82] and graphical shape [83]-[85]. Fluorescence code is not proper to scanner-based imaging. Color codes can be damaged after colorimetric assay and have limits on extending code with various scanners. The size the codes can make an influence on biochemical reaction during the assay. With different form, physical movement can be differed by the different buoyancy of different codes [82]. Graphical shape codes are selected as encoding strategy with the same size. Also, the shape of the total particle is the same to make same buoyancy of particles. These graphical shape codes have high multiplexing capacity with guaranteeing similar floating movements in suspension assay steps.

As an aligning key, rectangular form is additionally attached to the encoding region (Figure 3-2 (b)). Upside down particles are not congruent to aligned particles because of asymmetric form derived from an aligning key. This align key can also be used for adjusting the rotation of the particles. The algorithm for adjusting overturning and rotation is noted in Section 3.4.

(a) Dual function = Higher sensitivity + Detectable with scanner



(b)

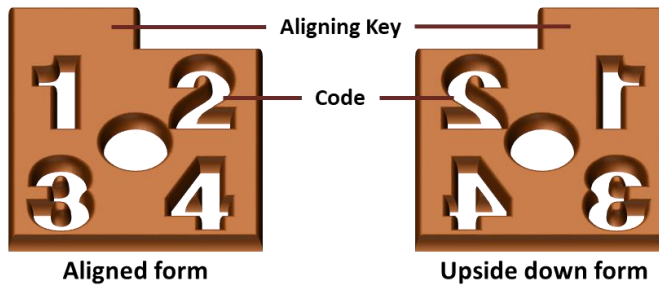


Figure 3.2 Schematic of $900 \mu\text{m}$ particles with character codes formed as holes. (a) Particles consist of two materials with different functions. One is a transparent part named as an analysis region which represents levels of target molecules as the color changes. The other is colored part named as an encoding region which indicates the target molecule. (b) The encoding region includes aligning key and code. The aligning key help to identify upside down form of the encoded particle.

The code region should be a hole or transparent form to be recognized well in scanned images. The encoding region consists of the colored polymer which can be detected well within widely spread office scanners. It is because office scanners are not proper imaging tools to distinguish transparent forms in high contrast. In the

same reason, the code should be a hole or transparent form to guarantee high contrast with colored regions. 900 μm particles have the code in a hole format (figure 3.2 (a)), and 300 μm particles have the code in a transparent format (figure 3.3).

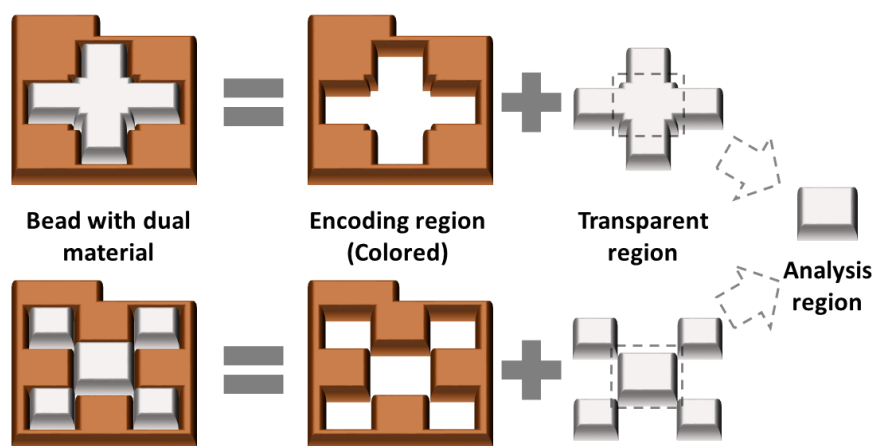


Figure 3.3 Schematic of 300 μm particles with binary codes formed as transparent regions. Particles consist of two materials with different colors. One is a transparent part, and the other is a colored part. The analysis region is not all transparent parts but only for centered transparent areas. It is because the transparent parts at the boundary show higher CV compared to the part at the center.

To perform an assay, the center region is more proper to get results in lower CV. At the edge of the particles show higher CV for colorimetric assay. So the analysis region is located at the center. To locate the assay regions at the center, laminar flow method [87] to fabricate particles which consist of several materials has not been selected.

To be imaged by an office scanner within the limited resolution, the size of the particle should be considered. Because of the limited resolution of scanners, the code of the particles in the microparticles is hard to be recognized by scanners in enough resolution. Besides, the analysis region should be large enough to get enough colored region to analyze in low CV. The size of microparticles and the resolution of scanners have a relation of negative correlation. So two kinds of size have been developed for this platform. 900 μ m particles and 300 μ m particles can be detected with enough pixels to be decoded and analyzed by 1 200 dpi and 4 800 dpi, respectively.

3.1.2. Fabrication process of dual-functional encoded particle

With the proper design of particles, the encoded particles should be fabricated with two functional materials. To fabricate particles in the intended shape, the photolithography technique is used. In the photolithography process, patterned UV light polymerizes at the specific region in which UV light is irradiated. With this property, the particles can be fabricated without a physical mold. Dual functions are integrated into a single particle by sequentially fabricating particle regions with different monomers.

To fabricate particles with various shapes, the photolithography method is used to polymerize in the intended shape. Chemical or thermal reaction can be used to fabricate the intended shape, but additional physical molds are necessary to fabricate each form. In photolithography, monomers can be polymerized with the

intended shape by irradiating patterned UV light [61]. This patterned UV light is irradiated by maskless lithography [28].

To fabricate dual-functional particle, polymerization is performed sequentially with two materials (figure 3.4). After the first polymerization, the polymerized particles are fixed on the glass substrate. So the firstly fabricated particle regions with the first monomer are fixed while washing not polymerized residue and loading the second monomer on the glass slide. Aligning the firstly fabricated particles then the second polymerization is performed. Finally, the polymerized dual functional particles are detached from the glass substrate by simply scrapping the surface of the substrate with a razor blade. To fix the polymers only on the glass slide, Polydimethylsiloxane (PDMS) coated slide glass is used. Particles were fabricated both with character codes and with binary codes (figure 3.5).

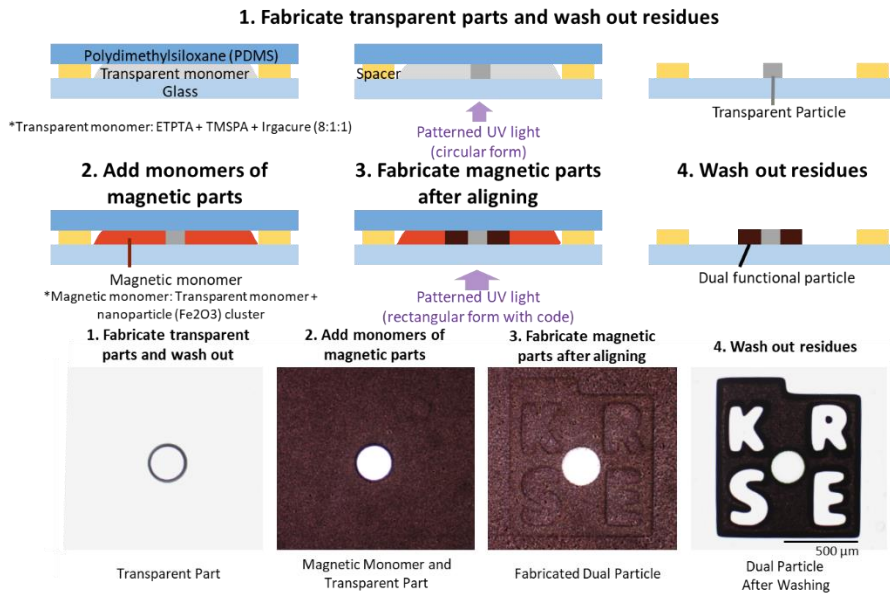


Figure 3.4 Schematic and images for showing fabrication process of dual-functional particles. $900 \mu\text{m}$ particles are fabricated with two different mixtures. The particles have codes in hole formats. The codes consist of 4 characters. The images are from microscopy [28].

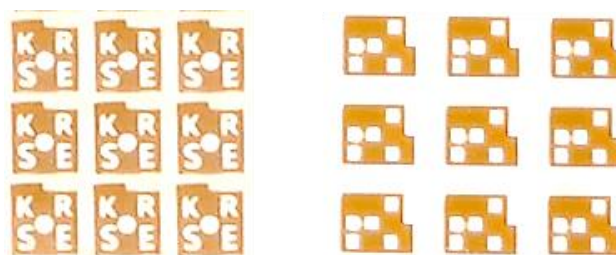


Figure 3.5 Scanned images of $900 \mu\text{m}$ encoded dual-functional particles. The particles have four-length character codes and eight-length binary codes respectively.

The materials for the particles are the mixture of monomers, photoinitiators, and iron nanoparticle clusters. Monomers are Trimethylolpropane ethoxylate triacrylate (ETPTA, $M_n = 428$) and 3-(trimethoxysilyl) propyl acrylate (TMSPA). Photoinitiator is Irgacure 1173. Nanoparticle cluster is Fe₃O₄ nanoparticles coated by polyacrylic acid (PAA) with approximately 80 nm [87]. Transparent monomer consists of ETPTA, TMSPA and Irgacure 1173 by 100:10:11 in volume. Colored monomer of 300 μm particle consists of the transparent monomer, and additionally, the nanoparticle clusters are added by 0.4% in weight. The colored monomer of 900 μm particle consists of ETPTA, Irgacure 1173 and nanoparticle clusters in the same ratio with the that of colored monomer for 300 μm particle, without TMSPA. The UV light is irradiated for 3 seconds within 35 mWcm^{-2} .

3.1.3. Strategy to fabricate dual-functional sequentially with fixing polymers at the same position.

To fabricate two kinds of monomer sequentially with two materials, the strategy is to fix the firstly fabricated polymer at the specific position of the substrate. Due to the fixation on the surface of the substrate, the firstly fabricated particles are not removed while washing and changing monomer for the second fabrication. If the substrate is aligned at the same position, the second polymerization can be induced at the same position so that the two materials with different functions can be integrated at a single particle.

To increase the physical bonding force between the firstly fabricated polymer

and the substrate, TMSPA (figure 3.6) is mixed in the monomer for the first fabrication. TMSPA are polymerized together with ETPTA. TMSPA makes the surface of the fabricated polymer to have functional groups which increase physical binding force to the glass substrate.

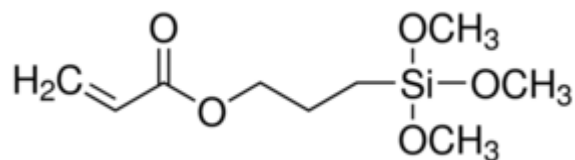


Figure 3.6 Condensed structure of TMSPA. The chemical groups including Si increase the physical bonding with glass substrates during polymerization.

Two different substrates are used to make polymer particles are fixed on the one substrate. One substrate is a glass slide on which the polymer particles are fixed with physical bonding, and the other substrate is PDMS-coated glass slide on which physical bonding is weak to be detached well. The PDMS layer on the substrate makes an oxygen layer (figure 3.7). The oxygen layer inhibits polymerization near the PDMS because O₂ is much more reactive compared to monomer [88]. So the physical bonding between PDMS and polymerized particles is weak enough to be detached easily after fabricating steps.

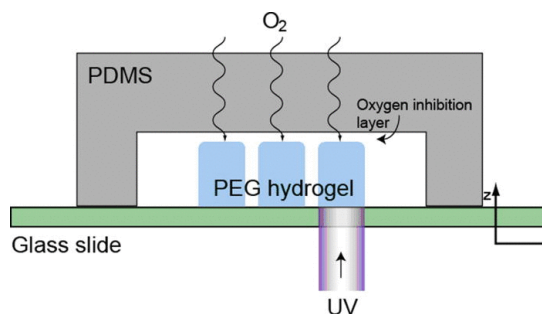


Figure 3.7 Schematic of oxygen inhibition layer derived near to PDMS during polymerization of PEG hydrogels. The oxygen layer is generated because PDMS is a gas permeable substrate. The oxygens absorb the chemically activated energy for polymerization, so the polymerization near the PDMS substrate is inhibited. Finally, the polymerized regions by UV light have weaker physical bonding force to PDMS substrate compared to the force to a glass substrate [88].

Transparent parts should be firstly fabricated to fix particles with higher bonding force. The magnetic nanoclusters can inhibit polymerization of the colored polymer. Also, the colored monomer mixture for the $900\ \mu\text{m}$ particles is not including TMSPA which increases physical bonding between polymers and glass substrates. Additionally, fabricating transparent particles guarantee enough areas for analyzing transparent regions.

3.1.4. High-throughput fabrication method

The particles should be prepared in a high-throughput manner for the platform to be used for the high-throughput assay. To make particles in a high-throughput

manner, the programmable motorized stage is used. However, the throughput still takes time, so a mask lithography technique is introduced to fabricate particles in high throughput. In the proof of concept, 1000 particles of $900 \mu\text{m}$ are fabricated in a few minutes. This throughput can be extended with a mask lithography technique.

The programmable motorized stage helps faster fabrication through maskless lithography [46], [62], [89]. The polymerization of the transparent monomer is sequentially performed at regular spatial intervals with programmed motorized stages. After several hundreds of transparent polymer particles are fabricated, residues which are not polymerized monomer are washed out and then colored monomer with the magnetic monomer is loaded. After aligning the substrate at the same position, the second polymerization of the colored monomer is performed (figure 3.8). With this method, hundreds of particles with dual polymers can be fabricated with changing monomers only once (figure 3.9).

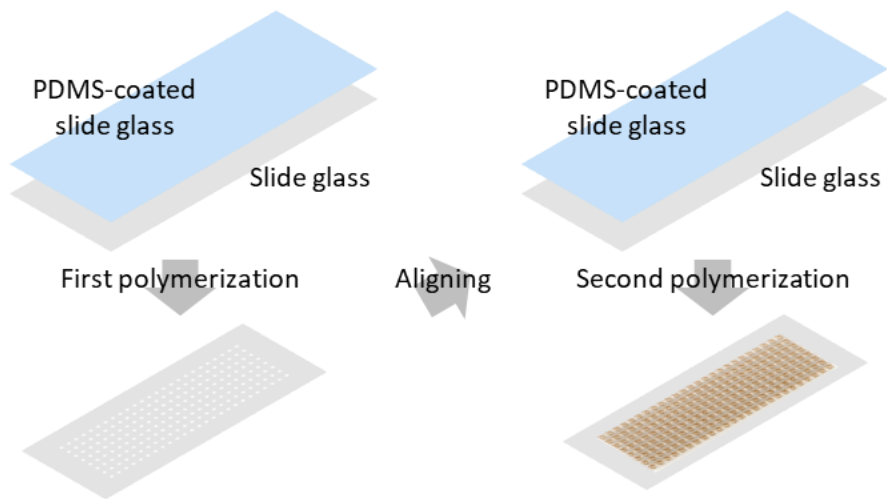


Figure 3.8 Schematic for process of sequential polymerization with a single monomer-changing step. Motorized stage and maskless lithography system is used for the polymerization steps.

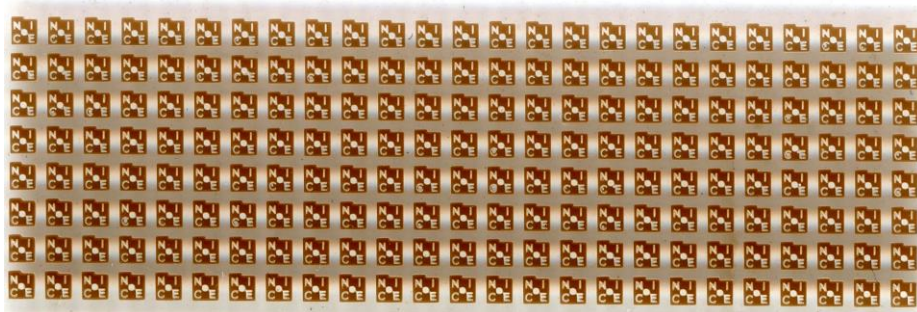


Figure 3.9 Scanned image of $900\ \mu\text{m}$ particles. Two hundred particles are fabricated with changing monomer only once. The particles are fabricated with the motorized stage.

The mask lithography is introduced to fabricate the encoded microparticles with dual materials in high-throughput in less than 3 minutes. For masking the light in order to make parallel UV light into intended patterned UV light, film combined glasses are used. The film combined glass is coated with PDMS in order to inhibit physical binding to the mask (figure 3.10). With PDMS coating the fabricated polymers can be physically bound to the glass substrate. For one code of dual-functional encoded microparticles, two film combined glasses are necessary. One is for fabricating a transparent part, and the other is for fabricating a colored part with magnetic nanoclusters. In this experiment, $900\ \mu\text{m}$ particles are fabricated in an array. The array is 25×38 so around 1,000 particles can be fabricated in one set of sequential two lithography steps. The mask has four regions for align key in the form of fractal structure (figure 3.10). These four regions are used to align the second mask glass with the glass substrate with firstly fabricated polymers. Using the aligning key, the mask glass and the glass substrate are roughly aligned and using a microscope, the two glasses are aligned perfectly.

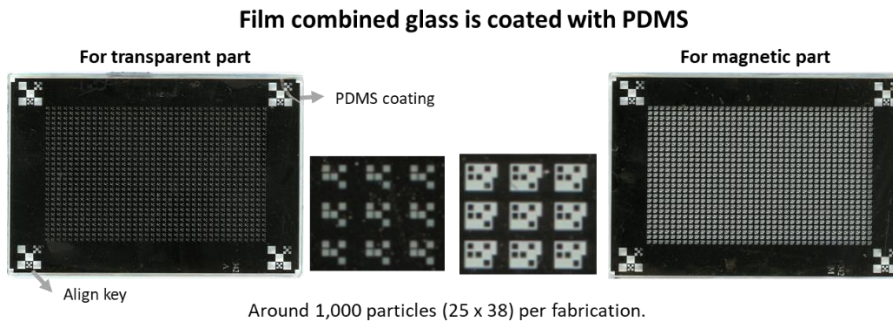


Figure 3.10 Images of film combined glasses for high-throughput mask lithography.

With rough alignment with four regions of fractal align keys, the fine alignment is performed with microscope images (figure 3.11, 3.12). The rough alignment is for pairing each transparent polymer to a single mask for fabricating the second polymer. With rough alignment, the arrays are paired correctly between the array of the firstly fabricated transparent polymers and the array of the second mask for generating the second patterned UV light. After aligning a top left polymer, a bottom right polymer is checked (figure 3.10). This alignment can assure that the angle of two substrates are aligned well, so the whole array is aligned correctly. After the checking, the two substrates are physically fixed. Then, the parallel UV light is irradiated through the second mask.

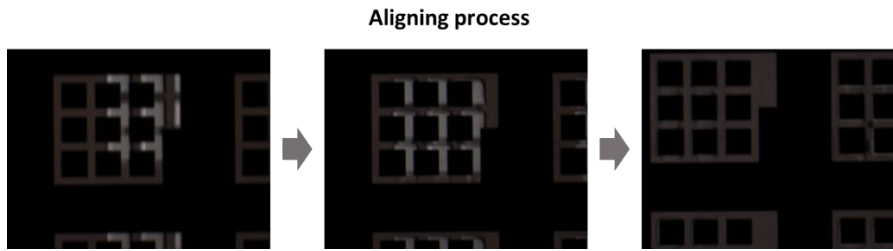


Figure 3.11 Aligning process using microscopy images. Using the align key, the mask and glass substrate is aligned roughly, so the mask array and the polymer array is well paired. The colored magnetic monomer and transparent polymer can be distinguished well by microscopy images. Delicate alignment is performed to adjust location and angle of paired sets of the second mask and the firstly fabricated polymer.

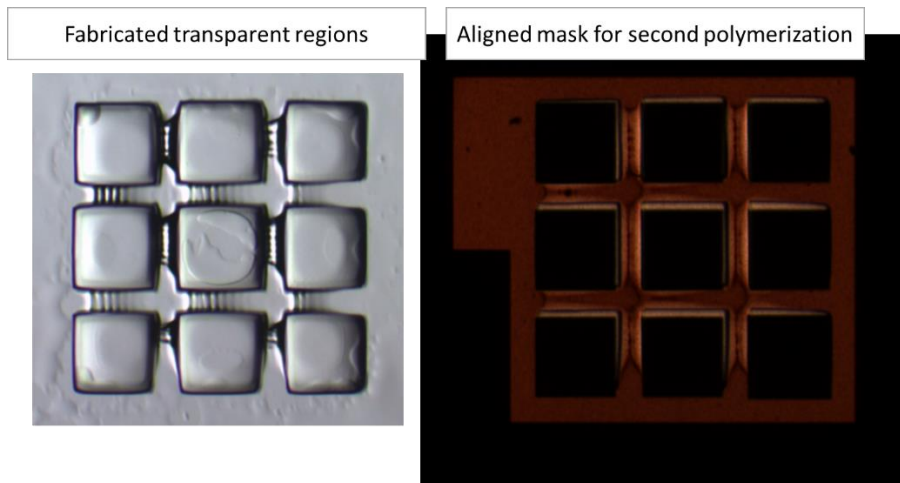


Figure 3.12 Microscope image of the firstly fabricated transparent polymer and the aligned set of the transparent polymer and the second mask.

With this alignment, around 1000 particles are fabricated in less than 3 minutes (figure 3.13). The monomer is changed only once, and UV light is irradiated only twice. The fabricated particles show uniform form. The uniformity of the fabricated particles is checked by scanning whole particles using an office scanner.

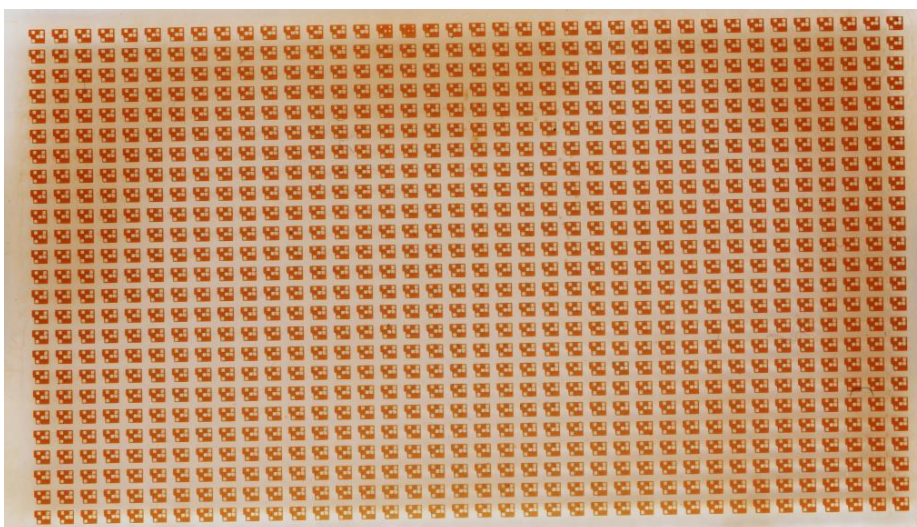


Figure 3.13 Scanned image of $900\ \mu\text{m}$ particles. One thousand particles are fabricated with two times of sequential irradiation of patterned UV light through film combined mask glass. The particles are fabricated with film mask and parallel irradiation of UV light.

Through the development of fabrication methods, time to fabricate particles in high-throughput is highly decreased as noted in table 3.1. Introducing a programmable motorized stage decreases the time spent in 12.5 times compared to fabricate particles one by one. Besides mask lithography technique decreases the

spending time more than 80 times compared to the spending time with a programmable motorized stage. Namely, the fabricating time decreases more than one thousand times compared to the time in one-by-one fabrication method.

Table 3.1 Comparison of fabricating time among the various fabrication methods.

Fabrication method	Time for fabricating 1 000 particles	Time for fabricating in the reasonable number of particles
Fabricate one by one	50 hours	3 minutes per one particle
Using motorized stage	4 hours	2 hours per 500 particles
Using mask lithography	< 3 minutes	3 minutes per > 1 000 particles (extendable)

3.1.5. Process of chemically conjugating capture molecules on surface of encoded particles

After two steps of polymerization, the encoded dual-functional particles should be conjugated with capture molecules to be used as a multiplex assay platform. The particles are firstly coated with silica. This silica coating inhibits unspecific binding of biomolecules to the particles [35]. Then, the functional groups of the silica surface are displaced with carboxyl groups. In the end, the carboxyl groups are chemically bound to the particles with ethyl- carbodiimide hydrochloride / N-hydroxysulfosuccinimide (EDC / surfo-NHS) reaction. All of these reactions can be performed in high-throughput. The particles and the reagents

are reacted in the 1.5 ml tube. The particles with each code are reacted separately and parallel.

The silica coating is performed by hydrolysis and condensation of tetraethyl orthosilicate (TEOS) to the TMSPA (figure 3.14). By incubated in TEOS solution, the polymerized particles are coated with silica groups. The role of TMSPA is to graft silane groups on the polymerized particles. To coat with silica groups, Stöber method is used in a modified version [62], [90].

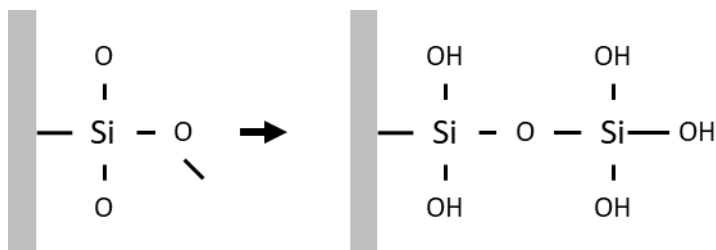


Figure 3.14 Silica coating process by the hydrolysis and the condensation of TEOS. The polymerized TMSPA is connected with the TEOS.

The coated silica groups are changed into amine groups and then into carboxyl groups [35]. The silica groups on the surface of the particles are functionalized into amine groups after incubated for 2 hours in the solution of 10% 3-triethoxysilylpropylamine (APTES) and EtOH solvent. Then, carboxyl groups are introduced from the amine groups after incubated for 2 hours twice in 6% gamma-butyrolactone (GBL) and 0.8% tris acetate-EDTA (TAE) in dimethylformamide (DMF) solvent.

Then the particles are coupled with aminylated capture molecules. Particles

are activated by incubating for 20 minutes at room temperature with 250 μ l activation buffer (50 mM 2-(N-morpholino)ethanesulfonic acid (MES) buffer, pH 6 with 50 mM EDC and 50 mM sulfo-NHS). Then particles are coupled with aminylated capture molecules for 30 minutes with 250 μ l coupling buffer (100 mM MES, pH6). Capture molecules for immunoassay were antigens and added in 8 μ g per 100 particles. Capture molecules for genotyping were reverse primers of targets. The washing step is included for two times with buffer for the next step, not including active molecules such as EDC, sulfo-NHS or capture molecules. After conjugating the encoded particles with aminylated capture molecules, the particles are washed three times with assay buffer (0.1 M phosphate buffer, pH 7.5 with 0.45 M NaCl, 3 wt% BSA, 1 wt% sucrose and 0.5 wt% Tween 20). Finally, the surface of the conjugated particles is blocked with bovine serum albumin (BSA). The silica coating and the chemical bonding are maintained higher than 100°C. So the particles conjugated with capture molecules can endure PCR process without denaturation.

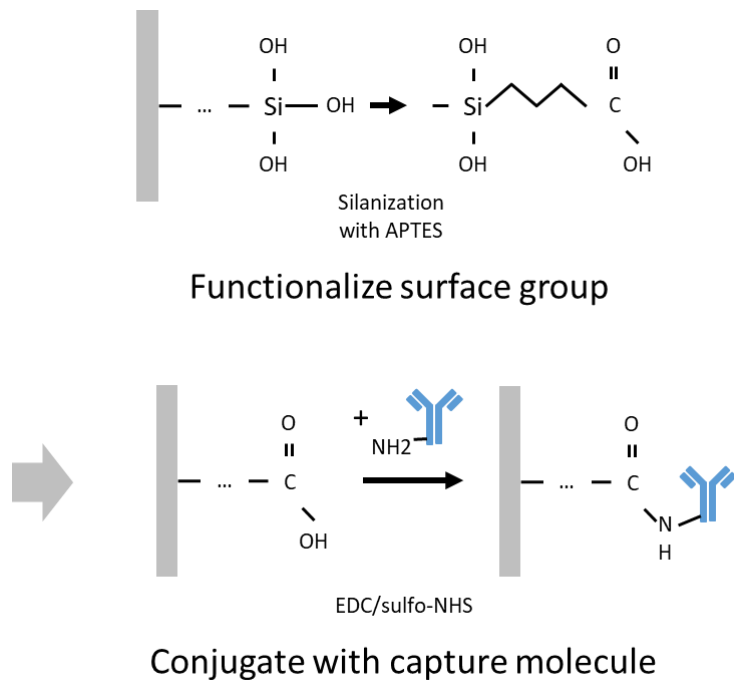


Figure 3.15 Steps and functional groups for conjugating aminylated capture molecules to the silica surface of the encoded microparticles. Silanization is performed with APTES, and conjugation step is based on EDC / surfo-NHS reaction which guarantees chemical bonding which endures high temperature more than 100°C.

3.2. Process of massively parallel multiplex colorimetric assay

Prepared encoded microparticles conjugated with capture oligos should be reacted with target biomarkers and detection molecules sequentially with additional washing steps. The encoded microparticles include Fe₃O₄ molecules in the encoding region, so with magnetic force, the particles are easily washed without

loss.

For immunoassay, the encoded microparticles conjugated with different capture proteins via codes are pooled in a 1.5 ml tube. The particles with the same codes are stored in assay buffer. The pooled particles are incubated with a sample for 30 minutes with shaking in room temperature. The particles are washed twice with the assay buffer. Then biotinylated detection antibodies were added at $3.2 \mu\text{g/ml}$. The biotinylated detection antibodies target and are conjugated with the whole target proteins fixed to the surface of the particles. The detection antibodies are incubated with the particles at room temperature with 30-minute shaking. After incubation, the particles are washed twice using assay buffer. Then, the anti-biotin gold nanoparticles are incubated with the particles at room temperature with 30-minute shaking. The anti-biotin gold nanoparticles are diluted in assay buffer to OD 1. Finally, the particles are ready for optical detection after washing with assay buffer three times.

3.3. Optimization of imaging process with office scanner

To be imaged in proper quality with an office scanner, optimizing the scanning condition is important. The scanner has fixed focus near the surface of the scanner and the options of resolution. Various plates have been tested with particles to find proper plates for assay and various resolutions have been tried to find a proper resolution for images which are decoded and analyzed well.

3.3.1. Optimization of imaging plate

Office scanners have a stationary focus to image the things located on the scanner. The plate for imaging should be checked if the focus is set well without blurring. The several plates have been checked if the scanned particles have the same pixels without blurring in the same resolution. The encoded particles are located on the scanner directly, on the thin cover glass, on the commercialized petri dish and the commercialized 96-well plate (figure 3.16). The 900 μ m particles are imaged with 400 dpi on the plates respectively. The pixels show similar quality in all plates except the 96-well plate. The scanned images of particles on a 96-well plate are blurred. In this dissertation, a petri dish is selected as a plate for imaging.



Figure 3.16 Images of 900 μm encoded particles on different plates. The particles are scanned in 400 dpi. Three images of particles except on 96-well plate show similar pixels for the area of the particles. The image of the particle on 96-well plate is blurred because the particle is located in the out of focus of the scanner.

3.3.2. Optimization of resolution of scanning

The resolution of the scanning is important to make the code decodable and to analyze the color change of the assay region with low CV. For analyzing the colorimetric assay results stably, it is determined to use more than 100 pixels to get an average RGB value from a single particle. The randomly assembled particles are not aligned well with the boundary of the pixels, so the resolution is selected to assure 100 particles roughly enough. For imaging 900 μm particles, 1 200 dpi is selected (figure 3.17), and for imaging 300 μm particles, 4 800 dpi is selected.

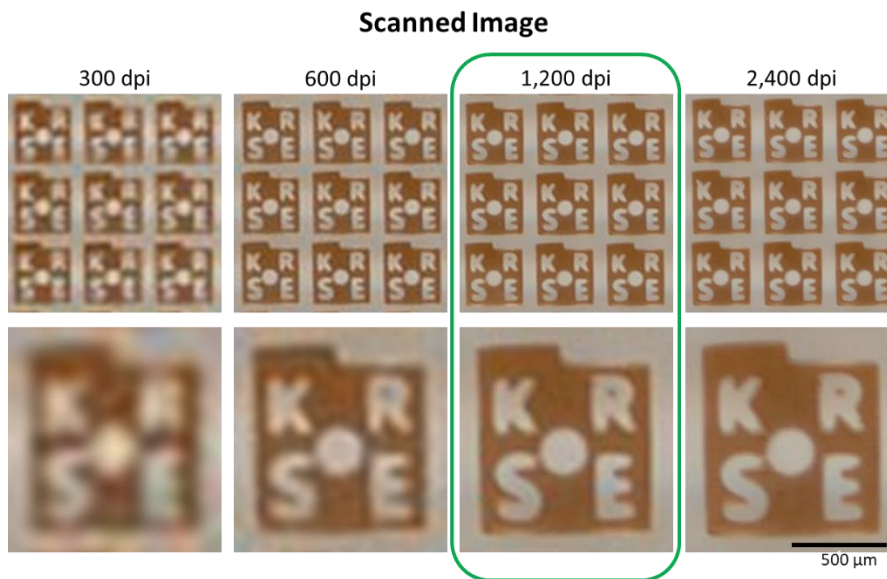


Figure 3.17 Scanned images of 900 μm particles with various resolution. For imaging 900 μm particles, the resolution of 1,200 dpi is selected as the most proper resolution in order to be decoded well and to use more than 100 pixels in analyzing colorimetric assay results [28].

3.4. Data analyzing process

After getting images from scanner, information should be extracted from the images. For the multiplex high-throughput assay, the images should be analyzed automatically. It has been studied in various ways to analyze integrated data in images. Mainly two kinds of information should be extracted. Firstly, the conjugated capture molecules to the encoded particles should be identified. Secondly, the levels of target molecules should be analyzed. The target molecules are captured by capture molecules and detected by detecting molecules. Through

the detecting molecules, the levels of target analytes are changed into color signals.

To analyze the integrated information in the scanned images of encoded microparticles, the encoded particles should be detected from the images, aligned by the intended orientation without upside-down form (figure 3.18), decoded with shape codes such as character codes or binary codes, and analyzed by the RGB value of the assay regions of the encoded particles.

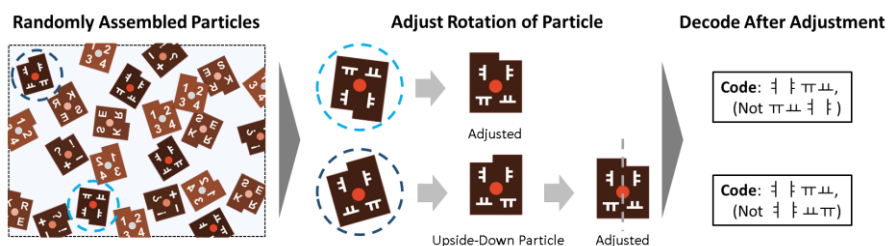


Figure 3.18 Algorithm of particle detection and decoding process. The detected particles can be upside-down and rotated due to a random assembly of the encoded particles. To decode correctly with various codes like ‘𐄂, 𐄃, 𐄄, 𐄅’ or ‘b, d, p, q,’ the particles should be appropriately oriented before character recognition process [28].

3.4.1. Particle detection and alignment process

The encoded dual-functional particle should be detected from the scanned images in which the encoded particles are randomly assembled on a transparent sheet. The particles are sometimes flipped and usually rotated. Using the image analysis, the similar forms to the encoded particles are detected. After detecting the encoded particles, then crop the images around the particles and save the cropped

images separately.

After detecting the encoded particles and cropping the images, the particles should be orientated properly from the cropped images to decode the character or binary codes. Also, the particles can be flipped and in that case, upside-down particles sometimes show different codes. Namely, particles should be adequately aligned without overturning to be decoded without error. For example, character codes such as ‘ㄷ, ㅌ, ㅍ, ㅑ’ and ‘b, d, p, q’ have different meanings if they are flipped or rotated. Also, for the binary code, the align key is necessary to indicate the position of the binary code.

To adjust the rotation and the overturning of the particles, align key has been as been integrated into the particles while designing particles. With this align key, the particle without overturning and the particle with overturning are asymmetric (figure 3.19). So the overturning can be distinguished and appropriately aligned to decode without error (figure 3.18). For adjusting the rotation of the particles, the distance is measured from the center of the particles (figure 3.19). The farthest point from the center is checked. Then, draw the line between the farthest point and the center of the particles. Then, check the distance to the edge of the particles with the same angle of the particles. With this, align the flipped particles, and adjust the rotation.

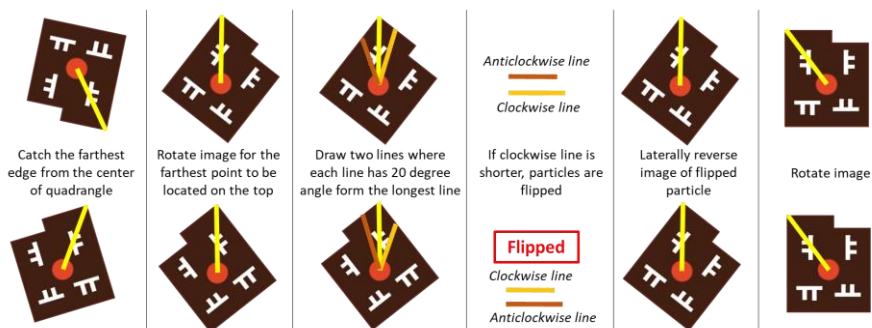
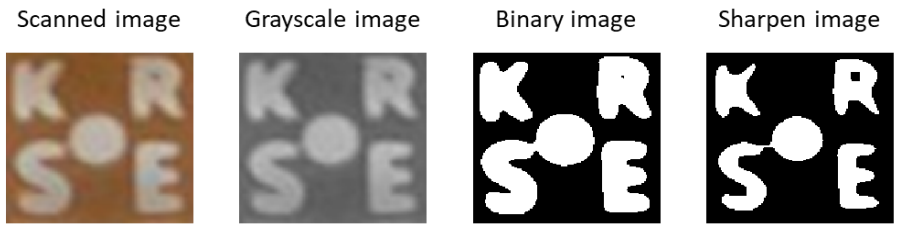


Figure 3.19 Algorithm for adjusting flipped or rotated particles. The center of an encoded microparticle is detected, and a line (yellow) is drawn toward the farthest edge of the particle. Two lines (red and orange) are drawn with the same angle to the edge from the center. The two lines are used to determine if the particles are flipped or not by comparing the length of two lines. Finally, the particles are oriented in a specific direction because the longest line (yellow) should be located in the left top [28].

3.4.2. Algorithm for decoding particles and analyzing results of colorimetric assay from scanned images

After detecting and aligning the particle images in a cropped form, the particle images should be decoded to identify capture molecules bound to the particles, and the colorimetric assay results should be analyzed from the RGB value from the assay region of the particles. The codes are character codes for $900 \mu\text{m}$ particles and binary codes for $300 \mu\text{m}$ particles. The character codes are modified into a binary image and decoded by optical character reader (OCR) code (figure 3.20).

The binary code has eight regions to be decoded as a 8-length binary code (figure 3.21). The eight regions for binary codes are positioned at the specific region of the particles which are guaranteed during the fabrication process. So the average RGB values of the eight regions are calculated from the intended specific areas. Each average RGB value from each specific area is compared with the mean value of the 8 RGB values from the eight specific areas. The spots with higher average RGB values are defined as a '1' region and the spots with lower medium RGB values are defined as a '0' region compared to the mean RGB value of the 8 RGB values.



Online optical character reader decodes as “K R S.E”

Figure 3.20 Image processing to read character codes in $900\ \mu\text{m}$ encoded particle. The scanned images are changed in grayscale images and then in binary images. After sharpening the images, the codes are read by the optical character reader.

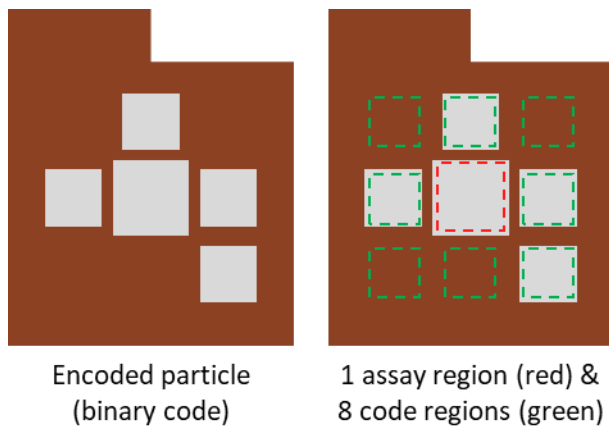


Figure 3.21 Schematic of $300\ \mu\text{m}$ binary particles and spots for a region for colorimetric assay in center and eight regions for binary codes.

For the binary codes, there can be decoding errors. To get higher decoding efficiency, the algorithm of error correction is necessary. In this dissertation, the error correction is performed to limit the number of ‘1’ areas. The number of ‘1’

areas is limited to only four areas. If there is a decoding error in calculating one binary spot to be wrongly decoded, the number of the '1' areas is changed into 3 or 5. Then, in the decoding algorithm, the particles having the different number of the '1' areas are treated as a wrongly decoded particle, and the decoding program saves the wrongly decoded images in a different folder and do not extract colorimetric data for the results. Although eight-length binary codes can have multiplexing capacity as 256, the eight-length binary codes with this error correction algorithm are limited to have the number of codes into 70 which is calculated by 8 combinations of 4.

Chapter 4. Platform validation with application: antibody from autoimmune disease and gene from bacterial meningitis

In this chapter, I describe the applications of the proposed platform with detecting antibodies and genes, as a proof of concept. Antibodies related to autoimmune disease are detected with 4-plex 900 μ m encoded particles. DNAs related to a bacterial meningitis disease are detected with 3-plex 300 μ m encoded particles.

4.1. Validation for immunoassay with autoimmune disease samples

To validate the platform as a screening platform of immunoassay, the platform has been applied to detect antibodies related to multiple sclerosis autoimmune disease [28]. In this experiments, four encoded microparticles are used to detect antibodies in the patient serum samples as proof of concept. The microparticles are chemically conjugated with antigens targeting antibodies related to the autoimmune disease. The 900 μ m encoded particles are used with four-length character codes (figure 4.1). The codes are including English alphabet, the Korean alphabet, number and other special marks such as question mark. The multiplexing capacity can be more than 2.5 million. The analytical sensitivity of the assay is 4 ng/ml. Autoantibodies targeting anoctamin 2 were detected to discriminate multiple sclerosis plasma samples from healthy control plasma samples. Two samples of human serum were discriminated $p < 0.0001$ using an unpaired t-test with an inter-assay % CV of 9.44% and a mean intra-assay % CV of 8.72%.

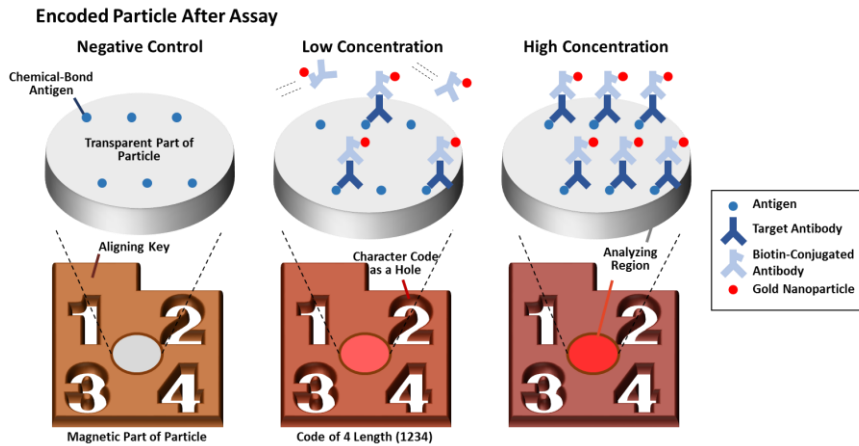


Figure 4.1 Schematic of immunoassay on encoded dual-function microparticle. The size of the particle is $900 \mu\text{m}$, and the particles are encoded with four lengths of character codes [28].

Three protein fragments and plasma samples were acquired from the Affinity Proteomics group at SciLifeLab, Royal Institute of Technology in Stockholm (KTH). The protein molecules have been produced within the Human Protein Atlas workflow. Two protein molecules, ANO2(1, 89 aa) and ANO2(2, 72aa), are representative amino acid sequences from the protein anoctamin 2. ANO2(1), but not ANO2(2) has been proven to be targeted by autoantibodies in multiple sclerosis plasma samples [91]. So the ANO2(1) is used as a positive control, and ANO2(2) is used as a negative control for the experiments. The other protein molecule is ZNF688 which is a representative protein fragment from zinc finger protein 688. This protein molecule has been proven as a common protein target for autoantibodies in healthy control as well [91]. So this protein is used as a second

negative control. Bovine serum albumin (BSA) is also used to be used as a negative control without any reaction to antibodies in samples. All these three protein molecules include a tag consisting of a hexahistidyl (His6) tag and an albumin binding protein (ABP). Rabbit anti-HisABP IgG was used to target these proteins which are acquired from the Human Protein Atlas.

The limit of detection was 4 ng/ml, and the dynamic range is 3 log, using ANO2(1) coupled particles and rabbit anti-HisABP IgG (figure 4.2). The rabbit anti-HisABP IgG is diluted in various concentrations with assay buffer. Then the various concentrations of the rabbit IgG are reacted with the ANO2(1) coupled microparticles. After washing steps, the microparticles are reacted with anti-biotin gold nanoparticles to change the levels of target molecules into optical color signals. Median color intensity (MCI) has been checked in arbitrary unit (AU) with scanned images. The concentration of the rabbit IgG and the MCI of assay regions show a linear correlation in 3 log scale from 4 ng/ml to 1000 ng/ml.

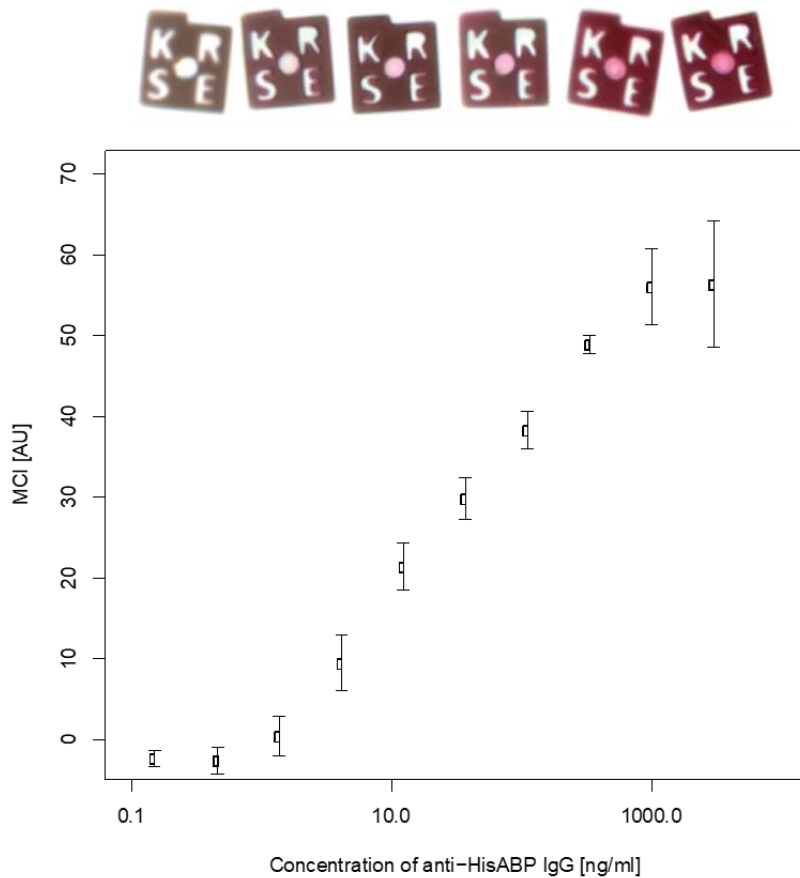


Figure 4.2 Plot and images to show the linear correlation between target concentration and color in scanned images. To check the color, median color intensity (MCI) is detected from the assay parts of the particles in scanned images of 1,200 dpi resolution. Rabbit anti-HisABP IgG is diluted in various concentrations using assay buffer. The results of the colorimetric assay were detected using anti-biotin gold nanoparticles and biotinylated goat anti-rabbit IgG which conjugate to encoded particles coupled with ANO2(1). MCI has an arbitrary unit, and error bars indicate \pm one intra-assay standard deviation [28].

As a proof of concept, human plasma samples are used. The samples used in these tests had been previously utilized in an autoimmunity study [91]. This experiment used 12 pooled plasma samples from multiple sclerosis autoimmune cases and 12 pooled samples from healthy controls. These plasma samples were collected during an epidemiological investigation of multiple sclerosis study in Sweden. In the process of investigation, target plasma samples were collected considering a population-based, case-control study. The total number of samples are 1063 for multiple sclerosis autoimmune cases and 1106 for healthy controls. The donors of the plasma samples were recruited between April 2005 and June 2011. The human participants of samples are varied in age and geographical areas in Sweden. The age is varied from 16 to 70 years. Incident cases were recruited at 40 clinical centers, including all university hospitals in Sweden. All participants were examined and diagnosed by a neurologist in 40 clinical centers and university hospitals. All donors fulfilled the McDonald criteria.

In purpose of testing the platform could distinguish multiple sclerosis plasma samples from healthy plasma samples, encoded microparticles were used which the codes can be distinguished by the shape of code within scanner images. Total four kinds of encoded microparticles were coupled with different proteins for multiplex assay. Each code indicates specific coating molecules which can be ANO2(1), ANO2(2), ZNF688 and BSA. These coupled particles were handled at once and incubated together with samples. The triplicate assay was performed and in each test at least 3 microparticles per code were reacted and analyzed (figure 4.3). The

color values, which were derived from scanned images of the microparticles coated with ANO2(1), were elevated significantly in the diseased samples compared to the healthy plasma samples with $p < 0.0001$ using an unpaired t-test (figure 4.4).

Prepared Particles

Encoded Particles	Coated With
	ANO2(1)
	ANO2(2)
	ZNF688
	BSA

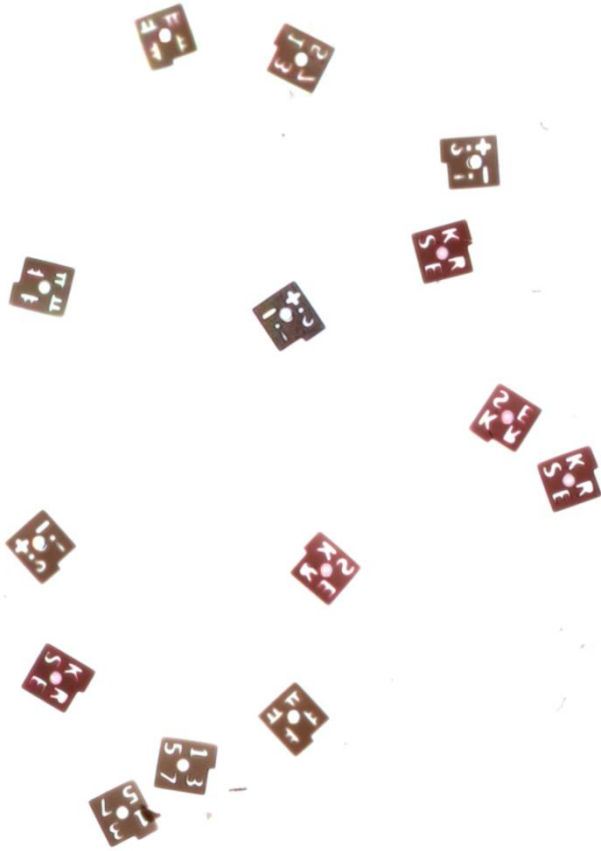


Figure 4.3 Schematic of encoded particles and scanned image of particles with four different codes which was conjugated with four different antigens. The particles were incubated with pooled multiple sclerosis plasma samples. The samples were diluted 250 times with assay buffer. The image was obtained using an office scanner, and scanning resolution was 1,200 dpi [28].

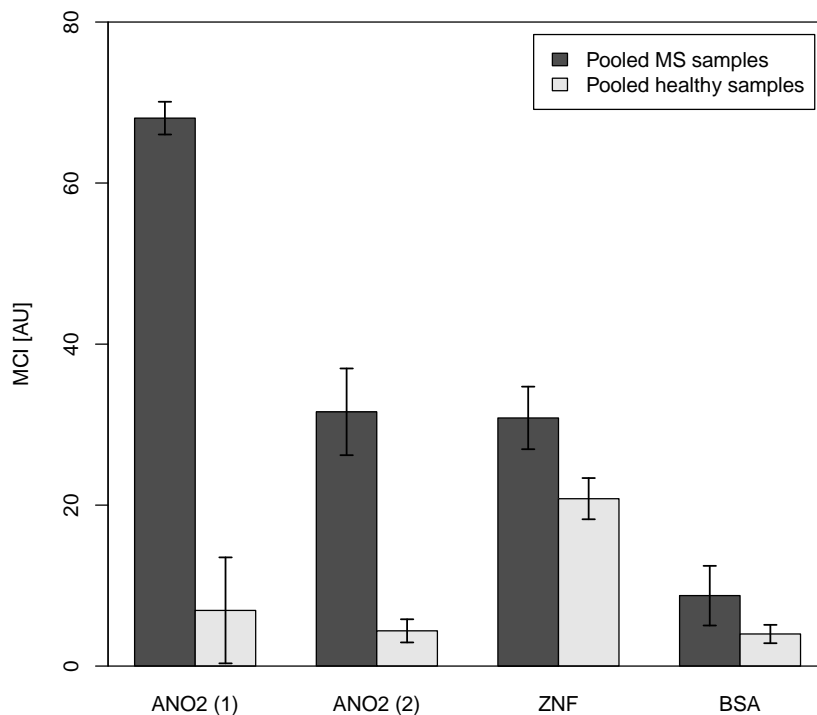


Figure 4.4 Plot to show the difference between pooled multiple sclerosis samples and pooled health samples. To check the color, median color intensity (MCI) is detected from the assay parts of the particles in scanned images of 1,200 dpi resolution. The microparticles with four different codes were conjugated with four different antigens. The particles were incubated with pooled multiple sclerosis plasma samples or pooled healthy plasma controls. The samples were diluted 250 times with assay buffer. Error bars indicate \pm one inter-assay standard deviation [28].

4.2. Validation for genotyping with bacterial meningitis target

Bacterial meningitis is one of the leading causes of death worldwide [23], [92]. Bacterial meningitis is in the sort of infectious diseases which makes impacts on large amount human populations directly or indirectly. The estimated incidence of bacterial meningitis per year is 1-2 cases per 100 000 people in developed countries [93]–[97]. The infections of bacterial meningitis in developing countries have not been calculated precisely because of the absence of accessible diagnostic tools but might be up to ten times higher in developing countries. The incidence is 1 000 cases per 100 000 people per year in the Sahel region of Africa [98]. The infectious diseases spread across geographical areas depending on the movement of infected human hosts without segregation. The movement of infected human hosts is derived by the late diagnosis or the low rate of the return visit. Besides, bacterial meningitis should be diagnosed rapidly and accurately because this bacterial meningitis is life-threatening disease compared to other meningitis derived from viruses or parasites [92]. Mortality of adult patients with bacterial meningitis is up to 30% [98]. Also, this bacterial meningitis is widely spread in developing countries. So the decentralized scanner-based platform with low-resource setting can be applied with highly advantaged.

The target DNAs are amplified together with encoded microparticles. So, the target DNAs are coupled on the encoded microparticles right after the assay without additional steps. The reverse primers are coupled on the encoded

microparticles. Biotinylated dUTPs have been added to be conjugated with anti-biotin gold nanoparticles for optical detection. The mixture for PCR consists of Qiagen PCR buffer with 2.5 units of DNA polymerase, 3mM MgCl₂, 300 μM dATP, 300 μM dGTP, 300 μM dCTP, 225 μM dTTP and 75 μM biotin-11-dUTP, 0.4 μM sodC forward primer, 0.1 μM sodC reverse primer, 0.5 μM lytA forward primer, 0.025 μM lytA reverse primer, samples with target templates and encoded particles conjugated with reverse primers. The total volume of the mixture is 50 μl. The PCR is performed for 40 cycles with 30 seconds in 94°C, 30 seconds in 60°C and 30 seconds in 72°C as well as 5 minutes in 95°C before the cycles and 10 minutes in 72°C after the cycles. After PCR and additional washing step, the particles are reacted with anti-biotin gold nanoparticles for 30 minutes in room temperature.

To improve the limit of detection, gold enhancement step is introduced to the assay [36]. The gold enhancement step amplifies the optical signal which is derived from detecting molecules. This method is based on physical principles. The larger the particles, the more optical signals are derived from light scattering and absorption in nanoscale volumes [99], [100]. This phenomenon is related to light scattering and surface Plasmon [101]. The seed nanoparticles are conjugated to the detecting molecules, and the size of the seed nanoparticles grow by the deposition of Au(0). By the deposition, the optical signals in a bright field increase proportional to the amount of scattered light due to the frequency of the Plasmon

resonance in the visible wavelength. This signal enhancement method has shown good concordance ($R^2 = 0.79 \pm 0.08$) compared to the conventional fluorescence detection [36].

The deposition of Au(0) on the seed gold nanoparticles is produced from Au(III) by the MES buffer and H₂O₂. With optimized concentrations of HAuCl₄, H₂O₂ and MES buffer as well as reaction pH, Au(0) is deposited on the seed nanoparticles. In 10 mM MES buffer pH 6, 5mM Gold(III) chloride (HAuCl₄·3H₂O) is mixed as the source of Au(III). Additionally, 1.027 M H₂O₂ is added to improve signal-to-noise ratio by promoting the formation of spherical gold structures. H₂O₂ slows down the synthesis of amorphous gold nanoparticles and finally promotes the deposition of Au(0) to the seed nanoparticles conjugated to the detecting molecules.

The multiplex assay with on-particle PCR has been performed and detected down to 1000 initial DNA molecules using gold nanoparticles (figure 4.5). The 1000 molecules have been detected with a signal enhancement step during 5 minutes. The 1000 initial target molecules have not been detected before depositing gold on the seed gold nanoparticles. The inter-particle CV was 12%.

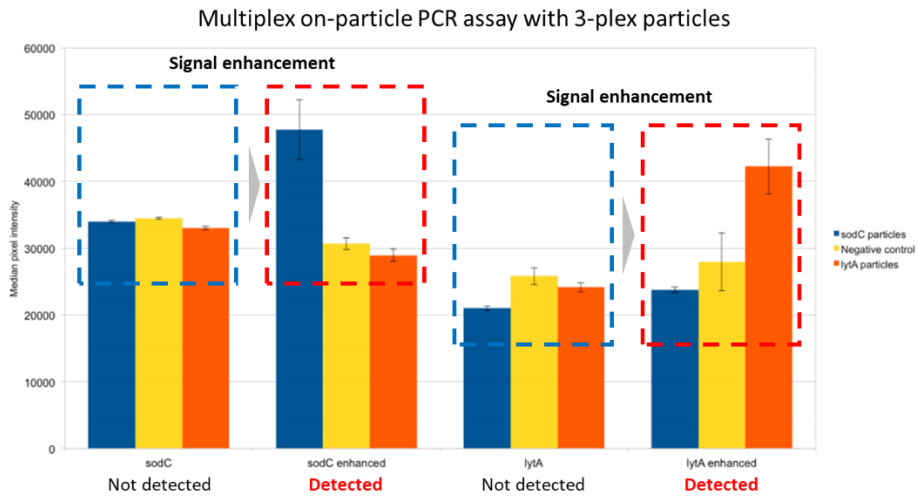


Figure 4.5 Median colorimetric intensity after performing 3-plex DNA detection from bacterial meningitis DNAs of 1 000 copies. Synthesized bacterial meningitis DNAs are diluted to have 1 000 copies in the solution. The particles are targeting sodC and lytA and negative control.

Chapter 5. Conclusion and Discussion

In this Chapter, the proposed platform is summarized. Then, the platform is compared to the conventional technique in the aspect of multiplexing capacity, throughput, and low-resource setting. In addition, the limit of this platform is described. Finally, future works that can make the platform closer to the patient are presented.

5.1. Summary of dissertation

In this dissertation, a new platform is proposed for colorimetric multiplex bead-based assay. In Chapter 3, the platform is developed and optimized through the process of the colorimetric multiplex bead-based assay. In Chapter 4, the platform is validated for immunoassay and genotyping. This platform is developed to detect assay result through a widely spread device, an office scanner. The novelty of this platform is to fabricate encoded particles with dual functions and to introduce signal enhancement step to the encoded microparticles using gold nanoparticles. This platform can be applied to various situations where operators need to perform the multiplex assay in high-throughput without high-resource settings. For example, with re-emerging of infectious diseases where the high resources have not been set, operators can perform the multiplex assay in high throughput within office scanners.

Two types of particles are developed in different specs (table 5.1) and applied to different applications. 300 μ m particles are used to detect antibodies and finally applied to discrimination of plasma from autoimmune disease patients. 900 μ m particles are used to detect genes and finally applied to detection of bacterial meningitis DNAs down to 1000 molecules.

Table 5.1 Spec of developed encoded particles in this dissertation.

Particle size	Code type	Multiplexing capacity	The number of particles in A4 scan	Scanning resolution
300 μ m	Binary	70-256	173,000	4,800 dpi
900 μ m	Character	>2,500,000	19,000	1,200 dpi

The encoded particles are fabricated with having two kinds of polymers which take different roles for multiplex colorimetric assay. The design of the encoded particles is considered to be detected with scanners without additional devices. The fabrication step has been developed to fabricate more than 1000 particles in several minutes using sequential polymerization with fixing and aligning strategies. The throughput of the fabrication can be extended in need.

Assay steps using two types of encoded microparticles (table 5.1) have been optimized for multiplex immunoassay and genotyping. Scanning condition, also, has been optimized with proper plate setting and resolution. Automated decoding and analyzing algorithms were proposed and developed. Codes are decoded to identify target molecules, and colorimetric assay results are analyzed according to the change of RGB values of transparent regions compared to negative controls. A five-minute signal enhancing step can decrease the limit of detection if it is needed. This step has been developed with introducing a gold deposition method to bead-based multiplex assay.

5.2. Comparison with previous technology

The colorimetric bead-based platform has advantages in multiplexing capacity, throughput, and low-resource setting. Multiplexing capacity is high compared to other previous methods because the bead-based assay has strength in increasing multiplexing capacity (figure 5.1). The detection process is performed by a widely spread device, an office scanner, so the platform has strength in a low-resource setting. Also, the high flexibility of the bead-based platform and the broad field of view of a scanner make the platform have high throughput to detect multiple analytes from a large amount of samples parallel.

	Colorimetric bead	Fluorescent bead	Paper	Array	Microfluidic
Accessibility	Decentralized but need manual work ●	Centralized (Fluorescence, Flow cytometry) ●	Decentralized ●	Decentralized but need many optimized setups ●	Decentralized but need minimal fluidics ●
Multiplex	70 – 2.5M, Extendable ●	50 – 500, Extendable ●	1 – 3, 5 ●	10 – 1M, Extendable ●	2, 5, 8 ●
Assay throughput	Very high ●	High ●	Very high ●	Medium ●	High ●
Chip prep. throughput	Very high ●	Very high ●	Low ●	Very low ●	Low ●
Sensitivity	High ●	Very high ●	Low ●	Very high ●	High ●
Resource setting	Scanner ●	Fluorescence, Flow cytometry ●	Eye, Phone, Scanner ●	Electrical setting or optical setting ●	Eye, Phone, Scanner ●
Operation	Operator ●	Highly educated operator ●	Very simple operation ●	Highly educated operator ●	Operator ●

● Very good ● Good ● Medium ● Bad ● Very bad

Figure 5.1 Comparable information and scoring of previously developed technology and colorimetric bead-based assay for multiplex point-of-care detection [40], [47], [54], [67]–[74].

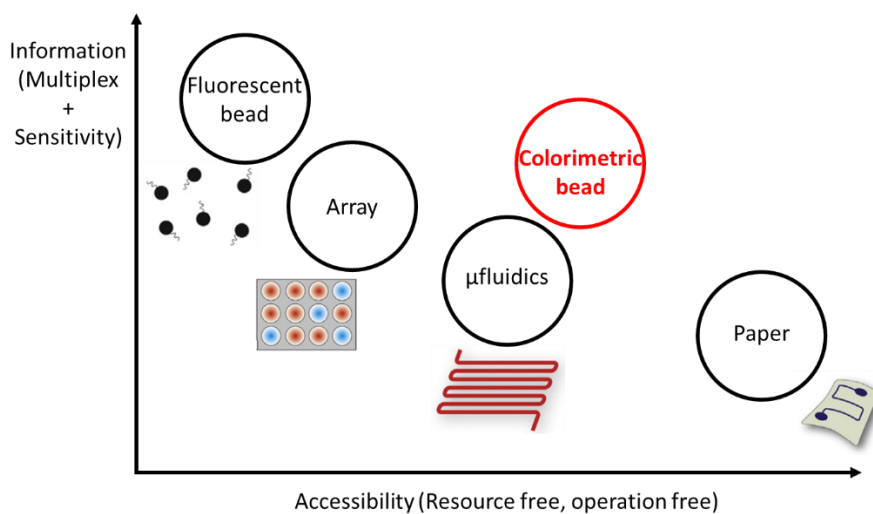


Figure 5.2 Positioning of colorimetric bead-based platform and other previous

platforms.

This platform with colorimetric bead-based assay is not operation-free but has advantages compared to other commercialized machines (figure 5.3). First of all, the conventional platforms with commercialized machines are not proper to low-resource settings. The machines are expensive ranging from \$40,000 to \$90,000. The scanner is much cheaper from \$50 to \$150 for 4,800 dpi which is the highest resolution used in this dissertation. Also, the scanner has been spread worldwide, so the detection platform does not have to be additionally set at many places having an office scanner. Besides, the price of the kits is lower. The companies compensate for the profit margin from kits, not from the devices. Also, the cost to fabricate kits is cheaper compared to kits for other devices. Especially Ella®, Verigene®, and Filmarray® utilize fully integrated cartridges for automatic sequential reactions. Ella® is not proper for expanding multiplex assay in high capacity because multiplexing limit is 4-plex. This system is more proper to applications testing one to four targets repetitively with high-throughput. Verigene® and Filmarray® are not proper for testing many samples in low-resource settings. The throughput of one machine is limited to only one sample in 1-2 hours. To test 100 patients per day with 8-16 hours working, 12 machines are necessary and the setting of devices costs around \$260,000 for Verigene® and around \$720,000 for Filmarray®. Although bead-based assay systems take operating labors and a long time for running and handling, the platforms of

Luminex fluorescent bead and this dissertation have high multiplexing capacity and throughput. It is because beads are flexible to be coupled respectively in parallel and pooled selectively.

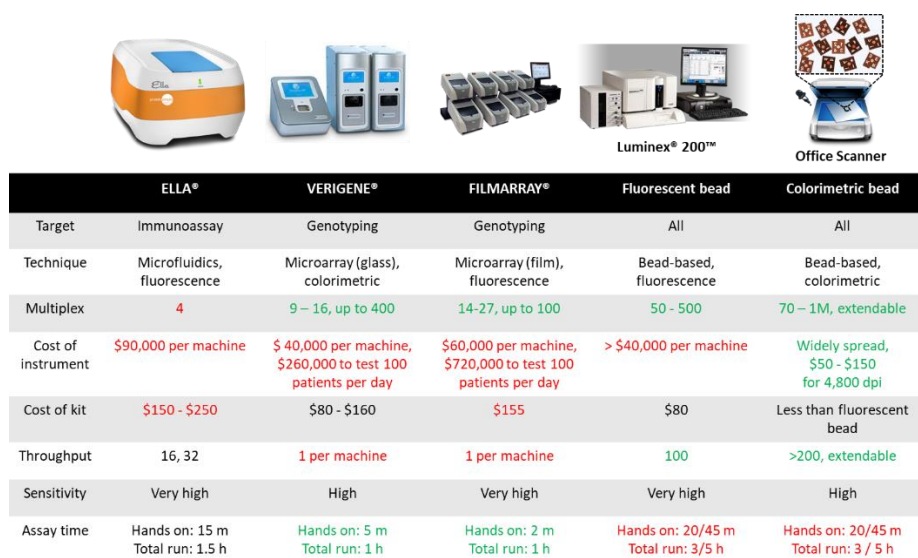


Figure 5.3 Comparison of proposed platform with commercialized set-ups. Pros are noted in green and cons are noted in red, to be applied to multiplex high-throughput assay within a low-resource setting. The images are devices noted below respectively.

5.3. Limit of platform

In the process of preparing samples, additional resource setting is necessary. For the validation as an immunoassay platform, patient plasma samples are used. However, to perform an assay using a whole blood sample, a centrifuge is necessary for extracting plasma from blood. However, the centrifuge costs around

\$100 with being able to centrifuge 2,000 rpm which is used for extracting plasma from blood. Also, the centrifuges are already spread to get samples to restore or deliver to centralized centers. In the validation as a genotyping platform, a PCR machine is used to amplify specific target DNAs. To substitute PCR machine, enzymes have been used for multiplex isothermal amplification of target genes [77], [102]. The amplified samples with some isothermal enzyme reactions can be applied to this system. For example, rolling circle amplification (RCA) and recombinase polymerase amplification (RPA) produce amplified DNAs which can be captured with encoded microparticles. The multiplex bead-based detection of isothermally amplified samples has already been shown in fluorescent detection [103], [104]. So this isothermal amplification can be applied to scanner-based multiplex assay to guarantee low-resource setting without PCR machines. However, in this dissertation, a PCR machine is used instead of isothermal amplification with enzymes.

This platform is not operation-free. Because the operating process is not fully automated, pipetting is necessary with operators. Operation process can be reduced by adding microfluidic technology. The microfluidic devices have already been developed to react and sort particles before imaging [105]. However, this platform has strength although the platform is not free from handful operations. The multiplex assay in high multiplexing capacity and throughput can be performed within operators who can perform biochemical reactions with pipetting and scanning with office scanners.

5.4. Future work

As mentioned in Section 5.3, a PCR machine is additionally used to genotyping applications in this dissertation. To guarantee as a platform performed within a low-resource setting, the platform will be applied to isothermally amplified targets. Among the many isothermal amplification methods [77], [102], RCA [106] and RPA [107] methods will be applied. RCA has high specificity because two regions should be reacted to target genes to be amplified. So RCA has advantages to be applied to multiplex amplification even compared to PCR. RPA is fast and labor-free with exponential amplification like PCR and one-step amplification without washing or changing temperature. So RPA can amplify targets faster than PCR. These amplified DNAs can be coupled to encoded microparticles, and colorimetric assay will be performed. Finally, the isothermally amplified targets can be detected by office scanners. Then, the multiplex genotyping can be performed within a scanner without additional PCR machines.

Bibliography

- [1] N. Patil, A. J. Berno, D. A. Hinds, W. A. Barrett, J. M. Doshi, C. R. Hacker, C. R. Kautzer, D. H. Lee, C. Marjoribanks, D. P. McDonough, B. T. N. Nguyen, M. C. Norris, J. B. Sheehan, N. Shen, D. Stern, R. P. Stokowski, D. J. Thomas, M. O. Trulson, K. R. Vyas, K. A. Frazer, S. P. A. Fodor, and D. R. Cox, “Blocks of limited haplotype diversity revealed by high-resolution scanning of human chromosome 21,” *Science* (80-.), vol. 294, no. 5547, pp. 1719–1723, 2001.
- [2] L. Ferrucci and J. M. Guralnik, “Inflammation, hormones, and body composition at a crossroad,” *American Journal of Medicine*, vol. 115, no. 6, pp. 501–502, 2003.
- [3] S. X. Leng, J. E. McElhaney, J. D. Walston, D. Xie, N. S. Fedarko, and G. A. Kuchel, “ELISA and multiplex technologies for cytokine measurement in inflammation and aging research,” *Journals of Gerontology - Series A Biological Sciences and Medical Sciences*, vol. 63, no. 8, pp. 879–884, 2008.
- [4] A. J. Atkinson, W. A. Colburn, V. G. DeGruttola, D. L. DeMets, G. J. Downing, D. F. Hoth, J. A. Oates, C. C. Peck, R. T. Schooley, B. A. Spilker, J. Woodcock, and S. L. Zeger, “Biomarkers and surrogate endpoints: Preferred definitions and conceptual framework,” *Clin. Pharmacol. Ther.*, vol. 69, no. 3, pp. 89–95, 2001.
- [5] D. Wild and E. Kodak, *The Immunoassay Handbook*. 2013.
- [6] C. Ramers, G. Billman, M. Hartin, S. Ho, and M. H. Sawyer, “Impact of a diagnostic cerebrospinal fluid enterovirus polymerase chain reaction test on patient management,” *J. Am. Med. Assoc.*, vol. 283, no. 20, pp. 2680–2685, 2000.
- [7] J. F. Rusling, C. V. Kumar, J. S. Gutkind, and V. Patel, “Measurement of biomarker proteins for point-of-care early detection and monitoring of cancer,” *Analyst*, vol. 135, no. 10, pp. 2496–2511, 2010.
- [8] S. D’Angelo, F. Mignone, C. Deantonio, R. Di Niro, R. Bordoni, R. Marzari, G. De Bellis, T. Not, F. Ferrara, A. Bradbury, C. Santoro, and D. Sblattero, “Profiling celiac disease antibody repertoire,” *Clin. Immunol.*, vol. 148, no. 1, pp. 99–109, 2013.
- [9] L. Anderon, “Candidate-based proteomics in the search for biomarkers of cardiovascular disease,” *Journal of Physiology*, vol. 563, no. 1, pp. 23–60, 2005.
- [10] S. Cheng, M. A. Grow, C. Pallaud, W. Klitz, H. A. Erlich, S. Visvikis, J. J. Chen, C. R. Pullinger, M. J. Malloy, G. Siest, and J. P. Kane, “A

- multilocus genotyping assay for candidate markers of cardiovascular disease risk,” *Genome Res.*, vol. 9, no. 10, pp. 936–949, 1999.
- [11] S. M. Grundy, “Metabolic syndrome: A multiplex cardiovascular risk factor,” *Journal of Clinical Endocrinology and Metabolism*, vol. 92, no. 2, pp. 399–404, 2007.
- [12] E. Halligan, J. Edgeworth, K. Bisnauthsing, J. Bible, P. Cliff, E. Aarons, J. Klein, A. Patel, and S. Goldenberg, “Multiplex molecular testing for management of infectious gastroenteritis in a hospital setting: a comparative diagnostic and clinical utility study.,” *Clin. Microbiol. Infect.*, vol. 20, no. 8, pp. O460–O467, 2013.
- [13] S. Spindel and K. E. Sapsford, “Evaluation of optical detection platforms for multiplexed detection of proteins and the need for point-of-care biosensors for clinical use,” *Sensors (Switzerland)*, vol. 14, no. 12, pp. 22313–22341, 2014.
- [14] J. Barenfanger, C. Drake, N. Leon, T. Mueller, and T. Troutt, “Clinical and financial benefits of rapid detection of respiratory viruses: An outcomes study,” *J. Clin. Microbiol.*, vol. 38, no. 8, pp. 2824–2828, 2000.
- [15] S. D. Goldenberg, M. Bacelar, P. Brazier, K. Bisnauthsing, and J. D. Edgeworth, “A cost benefit analysis of the Luminex xTAG Gastrointestinal Pathogen Panel for detection of infectious gastroenteritis in hospitalised patients,” *J. Infect.*, vol. 70, no. 5, pp. 504–511, 2015.
- [16] S. M. Hanash, S. J. Pitteri, and V. M. Faca, “Mining the plasma proteome for cancer biomarkers,” *Nature*, vol. 452, no. 7187, pp. 571–579, 2008.
- [17] V. Kulasingam and E. P. Diamandis, “Strategies for discovering novel cancer biomarkers through utilization of emerging technologies,” *Nature Clinical Practice Oncology*, vol. 5, no. 10, pp. 588–599, 2008.
- [18] A. M. Hawkridge and D. C. Muddiman, “Mass Spectrometry-Based Biomarker Discovery: Toward a Global Proteome Index of Individuality,” *Annu. Rev. Anal. Chem.*, vol. 2, no. 1, pp. 265–277, 2009.
- [19] D. R. Walt, “Miniature analytical methods for medical diagnostics,” *Science*, vol. 308, no. 5719, pp. 217–219, 2005.
- [20] World health organization, “Integrated Management of Hiv , Hcv , Tb and Other Coinfections,” *World Heal. Organ. Rep.*, no. January, 2018.
- [21] C. A. Holland and F. L. Kiechle, “Point-of-care molecular diagnostic systems – Past, present and future,” *Curr. Opin. Microbiol.*, vol. 8, no. 5, pp. 504–509, 2005.
- [22] S. S. Morse, “Factors in the emergence of infectious diseases,” *Emerg. Infect. Dis.*, vol. 1, no. 1, pp. 7–15, 1995.

- [23] D. M. Morens, G. K. Folkers, and A. S. Fauci, “The challenge of emerging and re-emerging infectious diseases.,” *Nature*, vol. 430, pp. 242–249, 2004.
- [24] World Health Organization, “World Health Organization. The Global Burden of Disease,” *World Health Organization. The Global Burden of Disease: 2004 Update.*, 2008. .
- [25] A. S. Fauci, “Infectious Diseases: Considerations for the 21st Century,” *Clin. Infect. Dis.*, vol. 32, no. 5, pp. 675–685, 2001.
- [26] R. Etzioni, N. Urban, S. Ramsey, M. McIntosh, S. Schwartz, B. Reid, J. Radich, G. Anderson, and L. Hartwell, “Early detection: The case for early detection.,” *Nat. Rev. Cancer*, vol. 3, no. 4, p. 243, 2003.
- [27] R. B., F.-S. N., C. J., V. R., D. J., M. F., G. F., B. Roson, N. Fernandez-Sabe, J. Carratala, R. Verdaguer, J. Dorca, F. Manresa, and F. Gudiol, “Contribution of a urinary antigen assay (Binax NOW) to the early diagnosis of pneumococcal pneumonia.,” *Clinical infectious diseases : an official publication of the Infectious Diseases Society of America*, vol. 38, no. 2. pp. 222–226, 2004.
- [28] G. Svedberg, Y. Jeong, H. Na, J. Jang, P. Nilsson, S. Kwon, J. Gantelius, and H. A. Svahn, “Towards encoded particles for highly multiplexed colorimetric point of care autoantibody detection,” *Lab Chip*, vol. 17, no. 3, pp. 549–556, 2017.
- [29] “ProteinSimple :: Powering Protein Research. A biotechne brand” [Online]. Available: <https://www.proteinsimple.com/>. Accessed November 2, 2018.
- [30] “bioMerieux, Inc. | In Vitro Diagnostics and Microbiology Testing Solutions.” [Online]. Available: <https://www.biomerieux-usa.com/>. Accessed November 2, 2018.
- [31] “Luminex Corporation | Biotechnology Engineering Company.” [Online]. Available: <https://www.luminexcorp.com/>. Accessed November 2, 2018.
- [32] M. J. Binnicker, “Multiplex molecular panels for diagnosis of gastrointestinal infection: Performance, result interpretation, and cost-effectiveness,” *J. Clin. Microbiol.*, vol. 53, no. 12, pp. 3723–3728, 2015.
- [33] R. Junker, H. Schlebusch, and P. B. Lippa, “Point-of-Care Testing in Hospitals and Primary Care,” *Dtsch. Aerzteblatt Online*, vol. 107, no. 33, 2010.
- [34] S. Sugama, K. Sekiyama, T. Kodama, Y. Takamatsu, M. Hashimoto, C. Bruno, Y. Kakinuma, M. Systems, C. Biology, and L. Jolla, “A Soft, Wearable Microfluidic Device for the Capture, Storage, and Colorimetric Sensing of Sweat,” *Sci Transl Med Sci*, vol. 8, no. 366, pp. 39–46, 2017.

- [35] L. N. Kim, M. Kim, K. Jung, H. J. Bae, J. Jang, Y. Jung, J. Kim, and S. Kwon, "Shape-encoded silica microparticles for multiplexed bioassays," *Chem. Commun.*, vol. 51, no. 60, pp. 12130–12133, 2015.
- [36] J. T. Dias, G. Svedberg, M. Nystrand, H. Andersson-Svahn, and J. Gantelius, "Rapid signal enhancement method for nanoprobe-based biosensing," *Sci. Rep.*, vol. 7, no. 1, pp. 1–8, 2017.
- [37] M. Zayats, R. Baron, I. Popov, and I. Willner, "Biocatalytic growth of Au nanoparticles: From mechanistic aspects to biosensors design," *Nano Lett.*, vol. 5, no. 1, pp. 21–25, 2005.
- [38] S. Wang, Z. Chen, J. Choo, and L. Chen, "Naked-eye sensitive ELISA-like assay based on gold-enhanced peroxidase-like immunogold activity," *Anal. Bioanal. Chem.*, vol. 408, no. 4, pp. 1015–1022, 2016.
- [39] R. P. Ekins, "Multi-analyte immunoassay *," vol. 7, no. 2, pp. 155–168, 1989.
- [40] C. Dincer, R. Bruch, A. Kling, P. S. Dittrich, and G. A. Urban, "Multiplexed Point-of-Care Testing – xPOCT," *Trends Biotechnol.*, vol. 35, no. 8, pp. 728–742, 2017.
- [41] K. Braeckmans, S. C. De Smedt, C. Roelant, M. Leblans, R. Pauwels, and J. Demeester, "Encoding microcarriers by spatial selective photobleaching," *Nat. Mater.*, vol. 2, no. 3, pp. 169–173, 2003.
- [42] Y. Song, Y. Jeong, T. Kwon, D. Lee, D. Y. Oh, T.-J. Park, J. Kim, J. Kim, and S. Kwon, "Liquid-capped encoded microcapsules for multiplex assays," *Lab Chip*, vol. 17, no. 3, pp. 429–437, Jan. 2017.
- [43] H. Lee, J. Kim, H. Kim, J. Kim, and S. Kwon, "Colour-barcoded magnetic microparticles for multiplexed bioassays," *Nat. Mater.*, vol. 9, no. 9, pp. 745–749, 2010.
- [44] Y. Jeong, Y. Song, and S. Kwon, "Rotating microcapsules for screening multiplexed and combinational assay in high-throughput," in *MicroTAS 2015 - 19th International Conference on Miniaturized Systems for Chemistry and Life Sciences*, 2015.
- [45] H. Fenniri, L. Ding, A. E. Ribbe, and Y. Zyrianov, "Barcoded resins: A new concept for polymer-supported combinatorial library self-deconvolution," *Journal of the American Chemical Society*, vol. 123, no. 33, pp. 8151–8152, 2001.
- [46] S. Han, H. J. Bae, J. Kim, S. Shin, S. E. Choi, S. H. Lee, S. Kwon, and W. Park, "Lithographically encoded polymer microtaggant using high-capacity and error-correctable QR Code for anti-counterfeiting of drugs," *Adv. Mater.*, vol. 24, no. 44, pp. 5924–5929, 2012.
- [47] N. R. Pollock, J. P. Rolland, S. Kumar, P. D. Beattie, F. Noubary, V. L. Wong, R. A. Pohlmann, U. S. Ryan, and M. Whitesides, "A paper-based multiplexed transaminase test for low-cost, point-of-care liver

- function testing,” *Sci. Transl. Med.*, vol. 4, no. 152, 2013.
- [48] T. Chinnasamy, L. I. Segerink, M. Nystrand, J. Gantelius, and H. A. Svahn, “A lateral flow paper microarray for rapid allergy point of care diagnostics.,” *Analyst*, vol. 139, no. 10, pp. 2348–54, 2014.
- [49] A. K. Yetisen, M. S. Akram, and C. R. Lowe, “Paper-based microfluidic point-of-care diagnostic devices,” *Lab Chip*, vol. 13, no. 12, pp. 2210–2251, 2013.
- [50] J. Hu, S. Q. Wang, L. Wang, F. Li, B. Pingguan-Murphy, T. J. Lu, and F. Xu, “Advances in paper-based point-of-care diagnostics,” *Biosens. Bioelectron.*, vol. 54, pp. 585–597, 2014.
- [51] S. J. Vella, P. Beattie, R. Cademartiri, A. Laromaine, A. W. Martinez, S. T. Phillips, K. A. Mirica, and G. M. Whitesides, “Measuring markers of liver function using a micropatterned paper device designed for blood from a fingerstick,” *Anal. Chem.*, vol. 84, no. 6, pp. 2883–2891, 2012.
- [52] J. D. Cortese, “The Array of Today,” *Sci.*, pp. 25–28, 2000.
- [53] T. Thorsen, S. J. Maerkl, and S. R. Quake, “Microfluidic Large-Scale Integration,” vol. 298, no. October, pp. 580–585, 2002.
- [54] L. Lafleur, D. Stevens, K. McKenzie, S. Ramachandran, P. Spicar-Mihalic, M. Singhal, A. Arjyal, J. Osborn, P. Kauffman, P. Yager, and B. Lutz, “Progress toward multiplexed sample-to-result detection in low resource settings using microfluidic immunoassay cards,” *Lab Chip*, vol. 12, no. 6, pp. 1119–1127, 2012.
- [55] Q. Feng, J. Sun, and X. Jiang, “Microfluidics-mediated assembly of functional nanoparticles for cancer-related pharmaceutical applications,” *Nanoscale*, vol. 8, no. 25, pp. 12430–12443, 2016.
- [56] S. He, Y. Zhang, P. Wang, X. Xu, K. Zhu, W. Pan, W. Liu, K. Cai, J. Sun, W. Zhang, and X. Jiang, “Multiplexed microfluidic blotting of proteins and nucleic acids by parallel, serpentine microchannels,” *Lab Chip*, vol. 15, no. 1, pp. 105–112, 2015.
- [57] J. Guo, C. M. Li, and Y. Kang, “Erratum to: PDMS-film coated on PCB for AC impedance sensing of biological cells[Biomedical Microdevices, (2014), DOI:10.1007/s10544-014-9872-2],” *Biomedical Microdevices*, vol. 16, no. 5, p. 687, 2014.
- [58] M. Lee, K. Lee, K. H. Kim, K. W. Oh, and J. Choo, “SERS-based immunoassay using a gold array-embedded gradient microfluidic chip,” *Lab Chip*, vol. 12, no. 19, pp. 3720–3727, 2012.
- [59] S. J. Oh, B. H. Park, G. Choi, J. H. Seo, J. H. Jung, J. S. Choi, D. H. Kim, and T. S. Seo, “Fully automated and colorimetric foodborne pathogen detection on an integrated centrifugal microfluidic device,” *Lab Chip*, vol. 16, no. 10, pp. 1917–1926, 2016.
- [60] S. R. Nicewarner-Peña, R. G. Freeman, B. D. Reiss, L. He, D. J. Peña, I. D. Walton, R. Cromer, C. D. Keating, and M. J. Natan,

- “Submicrometer metallic barcodes,” *Science (80-.)*, vol. 294, no. 5540, pp. 137–141, 2001.
- [61] S. W. Song, Y. Jeong, and S. Kwon, “Photocurable polymer nanocomposites for magnetic, optical, and biological applications,” *IEEE J. Sel. Top. Quantum Electron.*, vol. 21, no. 4, pp. 1–14, 2015.
- [62] H. J. Bae, S. Bae, C. Park, S. Han, J. Kim, L. N. Kim, K. Kim, S. H. Song, W. Park, and S. Kwon, “Biomimetic microfingerprints for anti-counterfeiting strategies,” *Adv. Mater.*, vol. 27, no. 12, pp. 2083–2089, 2015.
- [63] I. D. Walton, S. M. Norton, A. Balasingham, L. He, D. F. Oviso, D. Gupta, P. A. Raju, M. J. Natan, and R. G. Freeman, “Particles for multiplexed analysis in solution: Detection and identification of striped metallic particles using optical microscopy,” *Anal. Chem.*, vol. 74, no. 10, pp. 2240–2247, 2002.
- [64] E. B. Cook, J. L. Stahl, L. Lowe, R. Chen, E. Morgan, J. Wilson, R. Varro, A. Chan, F. M. Graziano, and N. P. Barney, “Simultaneous measurement of six cytokines in a single sample of human tears using microparticle-based flow cytometry: Allergics vs. non-allergics,” *J. Immunol. Methods*, vol. 254, no. 1–2, pp. 109–118, 2001.
- [65] R. T. Carson and D. A. A. Vignali, “Simultaneous quantitation of 15 cytokines using a multiplexed flow cytometric assay,” *J. Immunol. Methods*, vol. 227, no. 1–2, pp. 41–52, 1999.
- [66] V. V. Krishnan, S. R. Selvan, N. Parameswaran, N. Venkateswaran, P. A. Luciw, and K. S. Venkateswaran, “Proteomic profiles by multiplex microsphere suspension array,” *J. Immunol. Methods*, vol. 461, no. July, pp. 1–14, 2018.
- [67] M. J. Bugugnani, “Triage® Cardiac Panel Biosite: Évaluation analytique,” *Immuno-Analyse et Biologie Specialisee*, vol. 15, no. 3, pp. 191–193, 2000.
- [68] A. L. Ghindilis, M. W. Smith, K. R. Schwarzkopf, K. M. Roth, K. Peyvan, S. B. Munro, M. J. Lodes, A. G. Stöver, K. Bernards, K. Dill, and A. McShea, “CombiMatrix oligonucleotide arrays: Genotyping and gene expression assays employing electrochemical detection,” *Biosens. Bioelectron.*, vol. 22, no. 9–10, pp. 1853–1860, 2007.
- [69] N. Reslova, V. Michna, M. Kasny, P. Mikel, and P. Kralik, “xMAP technology: Applications in detection of pathogens,” *Frontiers in Microbiology*, vol. 8, no. JAN. 2017.
- [70] S. A. Dunbar, “Applications of Luminex® xMAP™ technology for rapid, high-throughput multiplexed nucleic acid detection,” *Clinica Chimica Acta*, vol. 363, no. 1–2, pp. 71–82, 2006.
- [71] P. K. Drain and N. J. Garrett, “The arrival of a true point-of-care molecular assay-ready for global implementation?,” *The Lancet*

- Global Health*, vol. 3, no. 11. pp. e663–e664, 2015.
- [72] C. D. Chin, T. Laksanasopin, Y. K. Cheung, D. Steinmiller, V. Linder, H. Parsa, J. Wang, H. Moore, R. Rouse, G. Umvilighozo, E. Karita, L. Mwambarangwe, S. L. Braunstein, J. Van De Wijgert, R. Sahabo, J. E. Justman, W. El-Sadr, and S. K. Sia, “Microfluidics-based diagnostics of infectious diseases in the developing world,” *Nat. Med.*, vol. 17, no. 8, pp. 1015–1019, 2011.
- [73] A. Kling, C. Chatelle, L. Armbrrecht, E. Qelibari, J. Kieninger, C. Dincer, W. Weber, and G. Urban, “Multianalyte Antibiotic Detection on an Electrochemical Microfluidic Platform,” *Anal. Chem.*, vol. 88, no. 20, pp. 10036–10043, 2016.
- [74] S. Nayak, A. Sridhara, R. Melo, L. Richer, N. H. Chee, J. Kim, V. Linder, D. Steinmiller, S. K. Sia, and M. Gomes-Solecki, “Microfluidics-based point-of-care test for serodiagnosis of Lyme Disease,” *Sci. Rep.*, vol. 6, 2016.
- [75] C. D. Chin, V. Linder, and S. K. Sia, “Commercialization of microfluidic point-of-care diagnostic devices,” *Lab Chip*, vol. 12, no. 12, pp. 2118–2134, 2012.
- [76] A. St John and C. P. Price, “Existing and Emerging Technologies for Point-of-Care Testing,” *Clin. Biochem. Rev.*, vol. 35, no. 3, pp. 155–67, 2014.
- [77] B. W. Buchan and N. A. Ledebor, “Emerging technologies for the clinical microbiology laboratory,” *Clin. Microbiol. Rev.*, vol. 27, no. 4, pp. 783–822, 2014.
- [78] J. J. Storhoff, A. D. Lucas, V. Garimella, Y. P. Bao, and U. R. Müller, “Homogeneous detection of unamplified genomic DNA sequences based on colorimetric scatter of gold nanoparticle probes,” *Nat. Biotechnol.*, vol. 22, no. 7, pp. 883–887, 2004.
- [79] S. M. Hwang, M. S. Lim, M. Han, Y. J. Hong, T. S. Kim, H. R. Lee, E. Y. Song, K. U. Park, J. Song, and E. C. Kim, “Comparison of xTAG respiratory virus panel and verigene respiratory virus plus for detecting influenza virus and respiratory syncytial virus,” *J. Clin. Lab. Anal.*, vol. 29, no. 2, pp. 116–121, 2015.
- [80] K. Pabbaraju, S. Wong, K. L. Tokaryk, K. Fonseca, and S. J. Drews, “Comparison of the luminex xTAG respiratory viral panel with xTAG respiratory viral panel fast for diagnosis of respiratory virus infections,” *J. Clin. Microbiol.*, vol. 49, no. 5, pp. 1738–1744, 2011.
- [81] J. Kim, S. Bae, S. Song, K. Chung, and S. Kwon, “Fiber composite slices for multiplexed immunoassays,” *Biomicrofluidics*, 2015.
- [82] D. Lee, A. C. Lee, S. Han, H. J. Bae, S. W. Song, Y. Jeong, D. Y. Oh, S. Cho, J. Kim, W. Park, and S. Kwon, “Hierarchical shape-by-shape assembly of microparticles for micrometer-scale viral delivery of two

- different genes,” *Biomicrofluidics*, vol. 12, no. 3, 2018.
- [83] S. W. Song, S. D. Kim, D. Y. Oh, Y. Lee, A. C. Lee, Y. Jeong, H. J. Bae, D. Lee, S. Lee, J. Kim, S. Kwon, “One-step generation of a drug-releasing hydrogel microarray-on-a-chip for large-scale sequential drug combination screening.” *Adv. Sci.*, p1801380, 2018.
- [84] D. Y. Oh, H. Na, S. W. Song, J. Kim, H. In, A. C. Lee, Y. Jeong, D. Lee, J. Jang, and S. Kwon, “ELIPatch, a thumbnail-size patch with immunospot array for multiplexed protein detection from human skin surface,” *Biomicrofluidics*, 2018.
- [85] S. W. Song, H. J. Bae, S. Kim, D. Y. Oh, O. Kim, Y. Jeong, and S. Kwon, “Uniform Drug Loading into Prefabricated Microparticles by Freeze-Drying,” *Part. Part. Syst. Character.*, 2017.
- [86] D. C. Appleyard, S. C. Chapin, R. L. Srinivas, and P. S. Doyle, “Bar-coded hydrogel microparticles for protein detection: Synthesis, assay and scanning,” *Nat. Protoc.*, vol. 6, no. 11, pp. 1761–1774, 2011.
- [87] J. Ge and Y. Yin, “Magnetically tunable colloidal photonic structures in alkanol solutions,” *Adv. Mater.*, vol. 20, no. 18, pp. 3485–3491, 2008.
- [88] L. Lin, Z. Gao, H. Wei, H. Li, F. Wang, and J. M. Lin, “Fabrication of a gel particle array in a microfluidic device for bioassays of protein and glucose in human urine samples,” *Biomicrofluidics*, vol. 5, no. 3, 2011.
- [89] S. Han, H. J. Bae, S. D. Kim, W. Park, and S. Kwon, “An encoded viral micropatch for multiplex cell-based assays through localized gene delivery,” *Lab Chip*, vol. 17, no. 14, pp. 2435–2442, 2017.
- [90] W. Stöber, A. Fink, and E. Bohn, “Controlled growth of monodisperse silica spheres in the micron size range,” *J. Colloid Interface Sci.*, vol. 26, no. 1, pp. 62–69, 1968.
- [91] B. Ayoglu, N. Mitsios, I. Kockum, M. Khademi, A. Zandian, R. Sjöberg, B. Forsström, J. Bredenberg, I. Lima Bomfim, E. Holmgren, H. Grönlund, A. O. Guerreiro-Cacais, N. Abdelmagid, M. Uhlén, T. Waterboer, L. Alfredsson, J. Mulder, J. M. Schwenk, T. Olsson, and P. Nilsson, “Anoctamin 2 identified as an autoimmune target in multiple sclerosis,” *Proc. Natl. Acad. Sci.*, 2016.
- [92] M. T. Fitch and D. van de Beek, “Emergency diagnosis and treatment of adult meningitis,” *Lancet Infect. Dis.*, vol. 7, no. 3, pp. 191–200, 2007.
- [93] A. Schuchat, K. Robinson, J. D. Wenger, L. H. Harrison, M. Farley, A. L. Reingold, L. Lefkowitz, and B. A. Perkins, “Bacterial Meningitis in the United States in 1995,” *N. Engl. J. Med.*, vol. 337, no. 14, pp. 970–976, 1997.
- [94] M. L. Durand, S. B. Calderwood, D. J. Weber, S. I. Miller, F. S. Southwick, V. S. Caviness, and M. N. Swartz, “Acute Bacterial

- Meningitis in Adults -- A Review of 493 Episodes," *N. Engl. J. Med.*, vol. 328, no. 1, pp. 21–28, 1993.
- [95] B. Khwannimit, P. Chayakul, and A. Geater, "Acute bacterial meningitis in adults: A 20 year review," *Southeast Asian Journal of Tropical Medicine and Public Health*, vol. 35, no. 4. pp. 886–892, 2004.
- [96] D. Vibha, R. Bhatia, K. Prasad, M. V. P. Srivastava, M. Tripathi, and M. B. Singh, "Clinical features and independent prognostic factors for acute bacterial meningitis in adults," *Neurocrit. Care*, vol. 13, no. 2, pp. 199–204, 2010.
- [97] I. O. Okike, S. Ribeiro, M. E. Ramsay, P. T. Heath, M. Sharland, and S. N. Ladhani, "Trends in bacterial, mycobacterial, and fungal meningitis in England and Wales 2004–11: An observational study," *Lancet Infect. Dis.*, vol. 14, no. 4, pp. 301–307, 2014.
- [98] F. McGill, R. S. Heyderman, S. Panagiotou, A. R. Tunkel, and T. Solomon, "Acute bacterial meningitis in adults," *The Lancet*, vol. 388, no. 10063. pp. 3036–3047, 2016.
- [99] G. Mie, "Sättigungsstrom und Stromkurve einer schlecht leitenden Flüssigkeit," *Ann. Phys.*, vol. 331, no. 8, pp. 597–614, 1908.
- [100] E. Prodan, C. Radloff, N. J. Halas, and P. Nordlander, "A Hybridization Model for the Plasmon Response of Complex Nanostructures," *Science (80-.)*, vol. 302, no. 5644, pp. 419–422, 2003.
- [101] X. Fan, W. Zheng, and D. J. Singh, "Light scattering and surface plasmons on small spherical particles," *Light: Science and Applications*, vol. 3. 2014.
- [102] O. Mayboroda, I. Katakis, and C. K. O'Sullivan, "Multiplexed isothermal nucleic acid amplification," *Anal. Biochem.*, vol. 545, no. January, pp. 20–30, 2018.
- [103] S. C. Chapin and P. S. Doyle, "Ultrasensitive multiplexed microRNA quantification on encoded gel microparticles using rolling circle amplification," *Anal. Chem.*, vol. 83, no. 18, pp. 7179–7185, 2011.
- [104] S. Liu, H. Fang, C. Sun, N. Wang, and J. Li, "Highly sensitive and multiplexed miRNAs analysis based on digitally encoded silica microparticles coupled with RCA-based cascade amplification," *Analyst*, 2018.
- [105] P. K. Yuen, M. Despa, C.-C. (Jim) Li, and M. J. Dejneka, "Microbarcode sorting device," *Lab Chip*, vol. 3, no. 3, p. 198, 2003.
- [106] J. Banér, M. Nilsson, M. Mendel-hartvig, and U. Landegren, "Signal amplification of padlock probes by rolling circle replication," vol. 26, no. 22, pp. 5073–5078, 1998.
- [107] O. W. Stringer, J. M. Andrews, H. L. Greetham, and M. S. Forrest, "TwistAmp (R) Liquid: a versatile amplification method to replace

PCR,” *Nat. Methods*, vol. 15, no. 5, pp. I–III, 2018.

국문 초록

본 학위 논문에서는 동시다발적으로 단백질이나 유전물질을 색변화를 통해 진단할 수 있는 플랫폼을 개발하였다. 본 플랫폼은 최종적으로 오피스 스캐너로 분석할 수 있기에 고가의 장비 없이 환자와 보다 가까운 곳에서 활용될 수 있는 기술이다. 코드화된 미세입자를 통해 한 샘플에서 동시에 여러 가지 진단을 가능하게 하였으며, 금 나노입자를 통해 분석 결과가 색 변화로 나타나 스캐너로 검출할 수 있도록 하였다. 해당 기술을 구현하기 위하여 미세입자를 두 가지 물질로 구성되도록 제작하였고 빠르게 대용량으로 제작하는 기술 역시 개발하였다. 또한 색변화로 적은 양의 물질을 검출할 수 있도록 신호 증폭 기술을 입자 기반 진단 기술에 적용하였다.

본 플랫폼을 개발하기 위해서 우선 표적 생체물질을 잡을 수 있는 코드화된 미세입자를 제작하였다. 스캐너로도 분석에 충분한 이미지를 얻을 수 있도록 크기와 물질 등의 디자인이 고려되었다. 본 미세입자를 3분 이내에 1000 개 이상 제작할 수 있는 방법 역시 개발하였다. 제작된 코드화된 미세입자는 표적 생체물질만을 붙잡을 수 있도록 실리카 코팅된 후 화학적으로 포획분자가 코드 별로 다르게 부착된다. 여러 물질을 표적하는 코드화된 미세입자들은 함께 섞인 뒤에 표적물질이

있는 샘플과 동시다발적으로 반응한다. 표적물질을 반응 시킨 후에는 표적물질의 존재를 색변화로 나타낼 수 있도록 미세입자에 부착된 표적물질에만 골드 나노파티클이 붙게 된다. 신호가 약한 경우 골드 나노파티클의 크기를 키우는 반응을 통해 신호를 증폭시켜 확인한다. 반응이 모두 끝난 이후 미세입자들은 스캐너로 관측이 되고, 이미지 처리를 통해 코드와 표적물질의 양에 따라 변화된 색변화를 분석한다. 코드는 표적 물질의 종류를 나타내고, 색변화는 표적물질의 존재 정도에 비례하여 나타난다. 미세입자의 크기는 스캐너의 해상도에 직접적으로 연관이 있으므로 1 200 dpi 에서 분석이 가능한 900 μm 미세입자와 4 800 dpi 에서 분석이 가능한 300 μm 미세입자를 개발하였다. 각 입자는 문자코드를 활용하여 250만 개 이상의 코드를 가질 수 있고, 2진법의 코드를 활용하여 70 에서 256 개의 코드를 가질 수 있도록 개발되었다.

본 플랫폼이 다양한 진단 상황에 적용될 수 있음을 보이기 위하여, 환자 샘플에서 자가면역질환 관련 항체를 검출하는 실험과 적은 양의 박테리아 뇌수막염 관련 유전체를 검출하는 실험을 진행하였다. 4 종류의 동시다발적 분석을 통해 자가면역 질환 환자와 건강한 사람을 비쌍체 t 검정에서 $p < 0.0001$ 로 구분할 수 있었으며, 3 종류의 동시다발적 분석을 통해 박테리아 뇌수막염 관련 유전체를 1 000 개까지 검출해낼 수 있었다.

본 플랫폼을 통해 동시다발적 진단 기술의 의료 혜택을 보다 널리 확장시킬 수 있을 것으로 기대된다. 본 플랫폼은 고가의 장비들이 구축되지 않은 환경에서도 스캐너만 있다면 구현될 수 있으며 많은 수의 표적 물질을 동시에 확인할 수 있고 병렬적으로 많은 샘플을 진단할 수 있도록 개발되었기 때문이다.

주요어: 색변화 기반 동시다발적 진단, 현장 진단 기술, 코드화된 미세입자, 스캐너, 면역 분석이나 유전형 분석을 통한 진단

학번: 2013-20880